



Sources and transport of particulate matter on an hourly time-scale in Invercargill

T. Ancelet
B. Trompetter

P. Davy

**GNS Science Consultancy Report 2015/50
March 2015**

DISCLAIMER

This report has been prepared by the Institute of Geological and Nuclear Sciences Limited (GNS Science) exclusively for and under contract to Environment Southland. Unless otherwise agreed in writing by GNS Science, GNS Science accepts no responsibility for any use of or reliance on any contents of this report by any person other than Environment Southland and shall not be liable to any person other than Environment Southland, on any ground, for any loss, damage or expense arising from such use or reliance.

Use of Data:

Date that GNS Science can use associated data: 1 January 2015

BIBLIOGRAPHIC REFERENCE

Ancelet, T.; Davy, P.; Trompetter, B. 2015. Sources and transport of particulate matter on an hourly time-scale in Invercargill, *GNS Science Consultancy Report 2015/50* 59 p.

CONTENTS

EXECUTIVE SUMMARY	V
1.0 INTRODUCTION	1
1.1 REQUIREMENT TO MANAGE AIRBORNE PARTICLE POLLUTION	1
1.2 IDENTIFYING THE SOURCES OF AIRBORNE PARTICLE POLLUTION	1
1.3 REPORT STRUCTURE	2
2.0 METHODOLOGY	3
2.1 DATA ANALYSIS AND REPORTING	6
3.0 INVERCARGILL MONITORING SITE AND SAMPLING METHODOLOGY	7
3.1 SITE DESCRIPTION	7
3.2 PARTICULATE MATTER SAMPLING AND MONITORING PERIOD	8
3.3 CONCEPTUAL PM ₁₀ RECEPTOR MODEL FOR INVERCARGILL	9
3.4 LOCAL METEOROLOGY AT THE FERNWORTH PRIMARY SCHOOL SITE	9
3.5 PM ₁₀ CONCENTRATIONS AT THE FERNWORTH PRIMARY SCHOOL SITE	10
4.0 RECEPTOR MODELING ANALYSIS OF PM₁₀ IN INVERCARGILL	17
4.1 COMPOSITION OF PM _{2.5} AND PM _{10-2.5}	17
4.2 SOURCE CONTRIBUTIONS TO PM ₁₀	20
4.3 TEMPORAL VARIATIONS IN SOURCE CONTRIBUTIONS	22
4.4 WEEKDAY/WEEKEND VARIATIONS IN SOURCE CONTRIBUTIONS	26
4.5 VARIATIONS IN SOURCE CONTRIBUTIONS WITH WIND DIRECTION	30
4.5.1 Biomass combustion	30
4.5.2 Motor vehicles	31
4.5.3 Crustal matter	31
4.5.4 Coarse and fine marine aerosol	32
5.0 DISCUSSION OF THE FERNWORTH PRIMARY SCHOOL RECEPTOR MODELING RESULTS	35
5.1 SOURCES OF PM ₁₀ AT FERNWORTH PRIMARY SCHOOL	35
5.1.1 Biomass combustion	35
5.1.2 Motor vehicles	36
5.1.3 Crustal matter	36
5.1.4 Marine aerosol	36
6.0 RECOMMENDATIONS	39
7.0 REFERENCES	40

FIGURES

Figure ES.1	Diurnal profiles of PM ₁₀ concentrations for each day of the week.....	v
Figure ES.2	Average source contributions to PM ₁₀ at Fernworth Primary School.	vi
Figure ES.3	Average hourly diurnal profile of the biomass combustion source.....	vii
Figure ES.4	Average hourly source contributions (µg m ⁻³) at Fernworth Primary School.....	viii
Figure 2.1	Location of the Invercargill monitoring site (★).....	4
Figure 2.2	Image of a typical fine Streaker filter after sampling.....	5
Figure 3.1	Location of the Environment Southland monitoring site at Fernworth Primary School (★).....	7
Figure 3.2	Aerial photo of the Environment Southland monitoring site and its immediate environs	8
Figure 3.3	Wind rose over the sampling period (June–August 2014).....	10
Figure 3.4	Daily PM ₁₀ concentrations at Fernworth Primary School.	11
Figure 3.5	Hourly PM ₁₀ concentrations at Fernworth Primary School.....	11
Figure 3.6	Diurnal profile of PM ₁₀ concentrations.....	12
Figure 3.7	Diurnal profiles of PM ₁₀ concentrations for each day of the week.....	13
Figure 3.8	Average PM ₁₀ concentrations for each day of the week.	13
Figure 3.9	Polar plot of PM ₁₀ concentrations.	14
Figure 3.10	Polar plots of PM ₁₀ concentrations by day of the week.....	15
Figure 4.1	PM ₁₀ source profiles at Fernworth Primary School.	21
Figure 4.2	Average source contributions to PM ₁₀ at Fernworth Primary School.	22
Figure 4.3	Temporal variations in source contributions to PM ₁₀ at Fernworth Primary School.	22
Figure 4.4	Average hourly diurnal profile of the biomass combustion source.....	23
Figure 4.5	Average hourly diurnal profile of the motor vehicle source.....	24
Figure 4.6	Average hourly diurnal profile of the crustal matter source.....	24
Figure 4.7	Average hourly diurnal profile of the coarse marine aerosol source.....	25
Figure 4.8	Average hourly diurnal profile of the fine marine aerosol source.....	25
Figure 4.9	Average hourly source contributions (µg m ⁻³) at Fernworth Primary School.....	26
Figure 4.10	Biomass combustion contributions (µg m ⁻³) by day of the week.....	27
Figure 4.11	Motor vehicle contributions (µg m ⁻³) by day of the week.	28
Figure 4.12	Crustal matter contributions (µg m ⁻³) by day of the week.	28
Figure 4.13	Coarse marine aerosol contributions (µg m ⁻³) by day of the week.....	29
Figure 4.14	Fine marine aerosol contributions (µg m ⁻³) by day of the week.	29
Figure 4.15	Polar plot of biomass combustion contributions.	30
Figure 4.16	Polar plot of motor vehicle contributions.....	31
Figure 4.17	Polar plot of crustal matter contributions.	32
Figure 4.18	Polar plot of coarse marine aerosol contributions.....	33
Figure 4.19	Polar plot of fine marine aerosol contributions.....	33
Figure 5.1	Marine aerosol concentrations in a number of New Zealand locations.	37

TABLES

Table 2.1	Standards, guidelines and targets for PM concentrations.	6
Table 4.1	Elemental concentrations in PM _{2.5} collected at Fernworth Primary School (1643 samples).....	18
Table 4.2	Elemental concentrations in PM _{10-2.5} collected at Fernworth Primary School (1643 samples).....	19

APPENDICES

A1.0	APPENDIX 1: ANALYSIS TECHNIQUES	45
A1.1	ELEMENTAL ANALYSIS OF AIRBORNE PARTICLES	45
	A1.1.1 Ion beam analysis	45
A1.2	BLACK CARBON MEASUREMENTS	50
A1.3	POSITIVE MATRIX FACTORISATION	51
	A1.3.1 PMF model outline	52
	A1.3.2 PMF model used	53
	A1.3.3 PMF model inputs	53
A1.4	DATASET QUALITY ASSURANCE	55
	A1.4.1 Mass reconstruction and mass closure	55
	A1.4.2 Dataset preparation	57
A2.0	APPENDIX 2: CORRELATION PLOTS	59

APPENDIX FIGURES

Figure A1.1	Particulate matter analysis chamber with its associated detectors.....	45
Figure A1.2	Schematic of the typical IBA experimental setup at GNS Science.	46
Figure A1.3	Typical PIXE spectrum for an aerosol sample analysed by PIXE.....	46
Figure A1.4	Typical PIGE spectrum for an aerosol sample.	47
Figure A1.5	PESA spectrum for an aerosol sample showing the hydrogen peak at 1.250 MeV.....	48
Figure A1.6	Elemental limits of detection for PIXE routinely achieved as the GNS IBA facility for air filters.....	50
Figure A2.1	Elemental correlation plot.	59

APPENDIX TABLES

Table A1.1	Proton scattering energies of various elements for a 2.5MeV proton beam.	48
-------------------	---	----

APPENDIX EQUATIONS

Equation A1.1	49
Equation A1.2	51
Equation A1.3	51
Equation A1.4	52
Equation A1.5	52
Equation A1.6	52
Equation A1.7	53
Equation A1.8	54
Equation A1.9	54
Equation A1.10	55
Equation A1.11	55
Equation A1.12	56
Equation A1.13	56
Equation A1.14	56

EXECUTIVE SUMMARY

This report presents an analysis of size-segregated particulate matter ($PM_{2.5}$ and $PM_{10-2.5}$) samples collected on an hourly time-scale at Fernworth Primary School on Pomona Street, Invercargill, from 5 June to 22 August 2014. This work was commissioned by Environment Southland to help understand the sources contributing to ambient particulate matter concentrations. The study was partially funded by an Envirolink grant from the Ministry of Business, Innovation and Employment.

The elemental composition of $PM_{2.5}$ and $PM_{10-2.5}$ over every hour was determined and the data were used as the basis for identifying the sources contributing to PM_{10} in Invercargill. The temporal patterns and trends of the contributing sources were then used to explain the observed PM_{10} concentrations at the monitoring site.

PM_{10} concentrations in Invercargill

Average hourly PM_{10} concentrations in Invercargill displayed a bimodal diurnal cycle, with concentrations peaking from 18:00–22:00. A smaller peak in concentrations also occurred from 8:00–10:00. This type of pattern is consistent across New Zealand and suggests that PM_{10} concentrations during the winter in Invercargill are not related to workday activities. This is particularly apparent from Figure ES.1, which shows that PM_{10} concentrations display the same diurnal profile, regardless of day of the week.

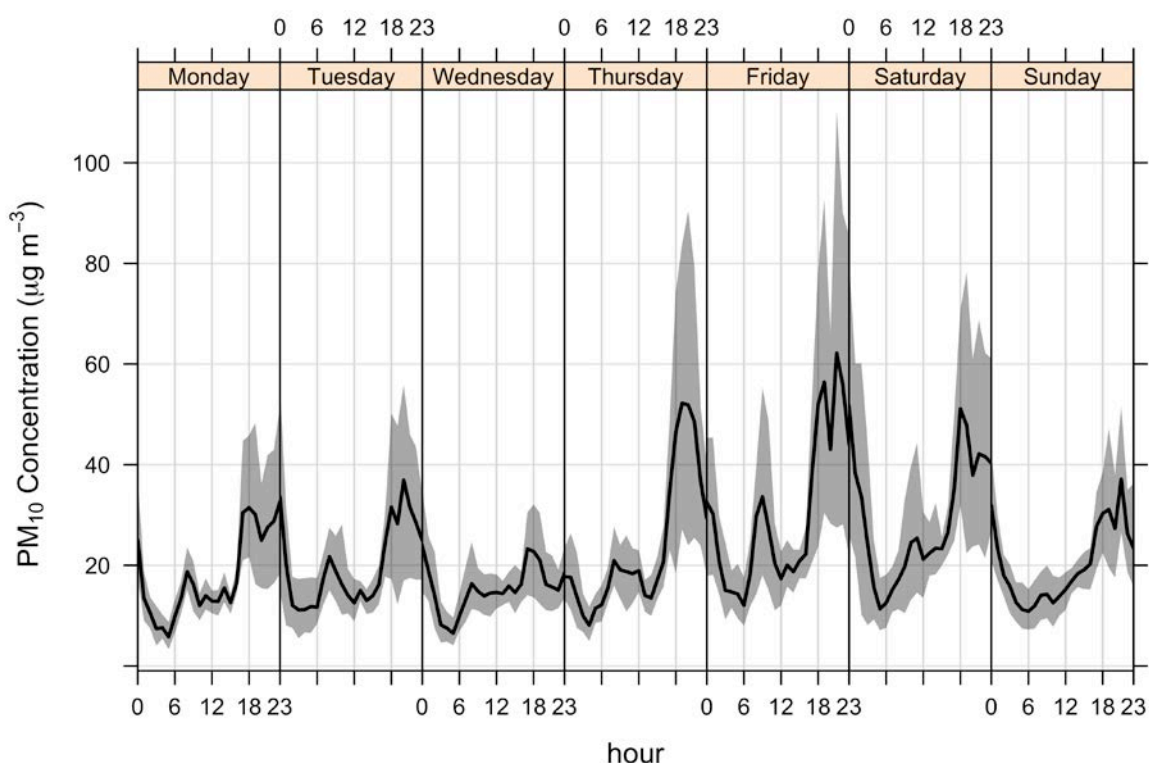


Figure ES.1 Diurnal profiles of PM_{10} concentrations for each day of the week. The solid dark lines indicate the average PM_{10} concentration and the shaded areas represent the 95% confidence intervals.

PM₁₀ sources in Invercargill

Five sources were extracted from the hourly elemental composition data using the positive matrix factorisation (PMF) receptor modeling technique. The sources were identified to be:

1. Biomass combustion;
2. Fine marine aerosol;
3. Crustal matter (soil);
4. Coarse marine aerosol;
5. Motor vehicles.

Figure ES.2 presents the relative contribution of each source to PM₁₀ concentrations. Elemental profiles for each of the sources identified have previously been established for other towns and cities across New Zealand.

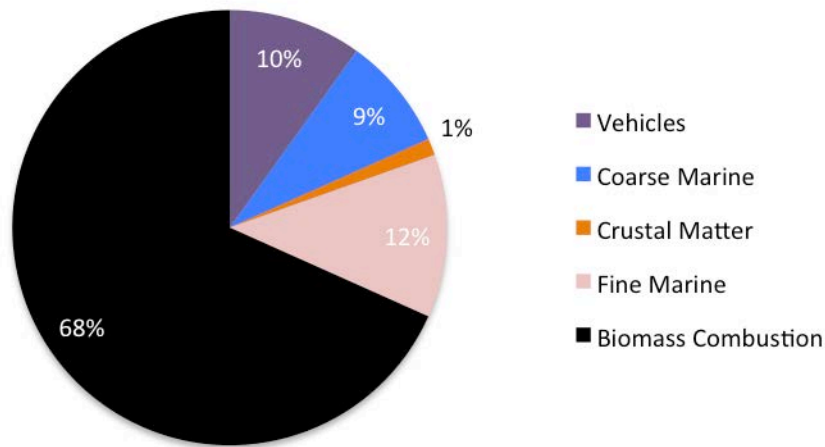


Figure ES.2 Average source contributions to PM₁₀ at Fernworth Primary School.

It is evident that biomass combustion is the dominant source contributor during the winter in Invercargill. Biomass combustion refers to emissions from solid fuel (primarily wood burning) combustion for home heating. While the biomass combustion source profile suggested that some coal burning may have occurred, emissions from wood burning were far higher and were most likely to lead to exceedances of the National Environmental Standard for Air Quality.

Biomass combustion

Biomass combustion was the dominant source contributor in Invercargill and displayed a bimodal diurnal pattern (Figure ES.3), with a large peak in contributions from 18:00–21:00 and a smaller peak from 7:00–9:00. This smaller peak suggests that residents are re-lighting their fires when they rise in the morning and is similar to other locations throughout New Zealand. Because of its dominant contribution, the biomass combustion diurnal profile closely matches that of PM₁₀.

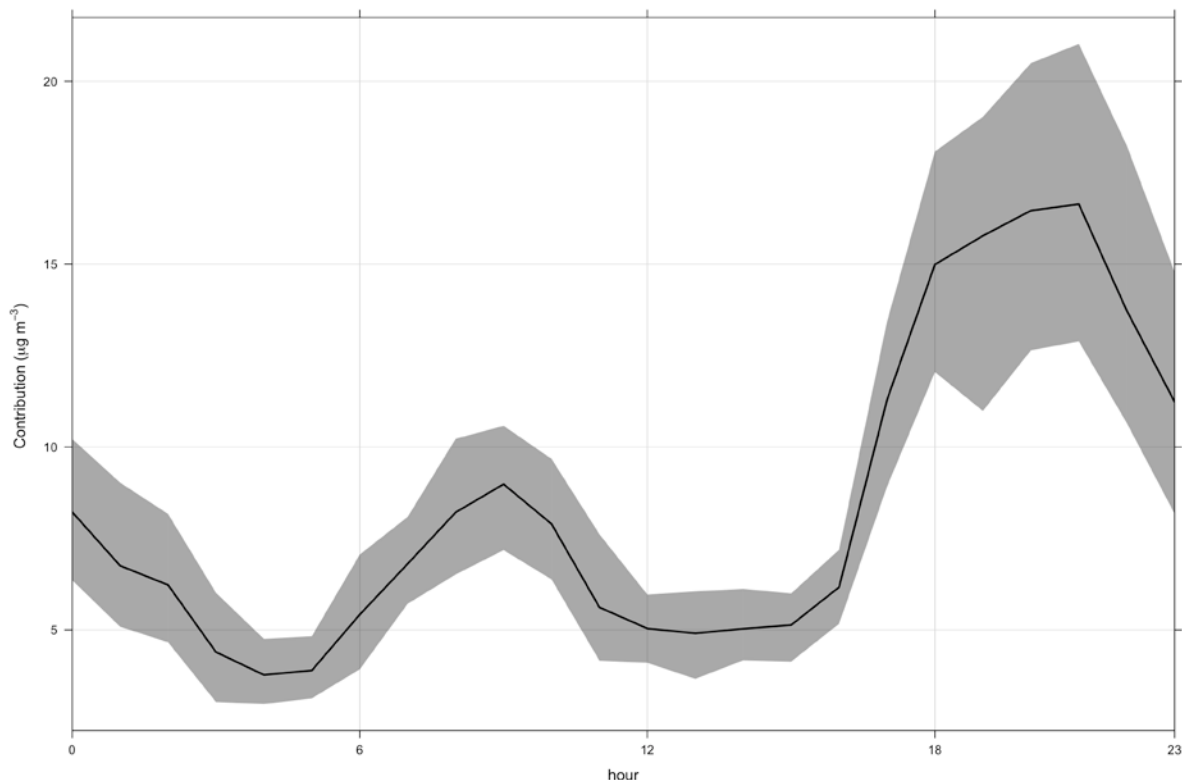


Figure ES.3 Average hourly diurnal profile of the biomass combustion source. The solid black line indicates the average concentration ($\mu\text{g m}^{-3}$) and the shaded area represents the 95% confidence intervals.

Biomass combustion contributions were found to peak under low wind speeds from the north. This indicates that katabatic flows under cold and calm anticyclonic synoptic meteorological conditions coupled with domestic fire emissions and poor dispersion were responsible for elevated biomass combustion contributions, similar to previous results in other New Zealand locations. Such meteorological conditions can reasonably be anticipated one or two days ahead of time so that it can be used as a predictor of high concentrations of particulate matter pollution from domestic fires or to issue warnings of an air pollution risk.

Arsenic and Lead associated with wood burning

The biomass combustion profile was found to incorporate arsenic and lead. These toxic elements are not typically found in wood combustion emissions around the world, but have been identified throughout New Zealand. Arsenic present in the biomass combustion profile is from residents burning copper chrome arsenate (CCA)-treated timber. Lead in the biomass combustion profile is most likely from residents burning lead-painted timber. Burning CCA-treated or lead-painted timber is likely intermittent and opportunistic, but it is clear that enough of these materials are entering the domestic fuel stream to have an impact on local air quality.

Motor vehicles

Emissions from motor vehicles were found to be a minor contributor to PM_{10} concentrations (10%). Contributions from vehicles did not show a weekday/weekend variation, suggesting that the monitoring site is not strongly influenced by commuter traffic. The relatively low influence of motor vehicles on PM_{10} concentrations is highlighted in Figure ES.4.

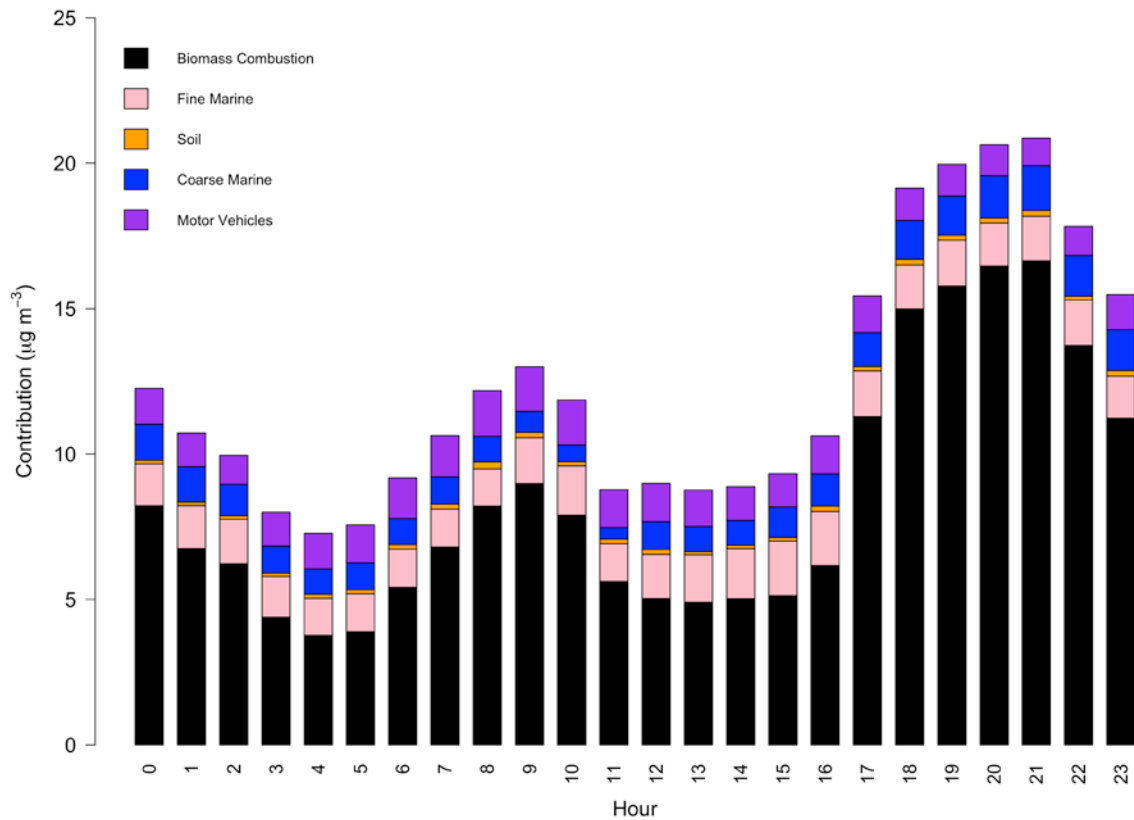


Figure ES.4 Average hourly source contributions ($\mu\text{g m}^{-3}$) at Fernworth Primary School.

Recommendations

Because biomass combustion has strong influence over PM_{10} concentrations in Invercargill, it is possible for Environment Southland to evaluate options for improving local air quality by targeting a reduction in biomass combustion for home heating. Even a small decrease in biomass combustion emissions should lead to an improvement in air quality. Since biomass combustion contributions were found to increase under cold, calm conditions, it may also be possible for Environment Southland to forecast high pollution days and take measures to mitigate emissions from home heating.

Given the presence of arsenic and lead contamination in PM_{10} and the link to domestic wood fires, Environment Southland may wish to consider monitoring campaigns to investigate the extent of the problem with a particular focus on residential locations where exposure is likely to be highest (i.e., neighbourhoods with a high percentage of domestic solid fuel fires).

1.0 INTRODUCTION

This report presents results from a receptor modeling study on hourly, size-segregated particulate matter samples collected in Invercargill. This work was commissioned by Environment Southland as part of their ambient air quality monitoring strategy and was partially funded by an Envirolink grant (1503-ESRC267) from the Ministry of Business, Innovation and Employment.

1.1 REQUIREMENT TO MANAGE AIRBORNE PARTICLE POLLUTION

In response to growing evidence of significant health effects associated with airborne particle pollution, the New Zealand Government introduced a National Environmental Standard (NES) in 2005 of $50 \mu\text{g m}^{-3}$ for particles less than $10 \mu\text{m}$ in aerodynamic diameter (denoted as PM_{10}). The NES places an onus on regional councils to monitor PM_{10} and publicly report if the air quality in their region exceeds the standard. Initially, regional councils were required to comply with the standard by 2013 or face restrictions on the granting of resource consents for discharges that contain PM_{10} , but the NES has since been revised, extending the target date for regional councils to comply with the standard. The new target dates are September 1, 2016 for airsheds with between 1 and 10 exceedances and September 1, 2020 for airsheds with 10 or more exceedances. In areas where the PM_{10} standard is exceeded, information on the sources contributing to those air pollution episodes is required to effectively manage air quality and formulate appropriate mitigation strategies.

In addition to the PM_{10} NES, the Ministry for the Environment issued ambient air quality guidelines for air pollutants in 2002 that included a guideline value of $25 \mu\text{g m}^{-3}$ for particles less than $2.5 \mu\text{m}$ in aerodynamic diameter ($\text{PM}_{2.5}$) (24-hour average). More recently, the World Health Organisation (WHO) has confirmed a $\text{PM}_{2.5}$ ambient air quality guideline value of $25 \mu\text{g m}^{-3}$ (24-hour average) based on the relationship between 24-hour and annual PM concentrations (WHO, 2006). The WHO annual average guideline for $\text{PM}_{2.5}$ is $10 \mu\text{g m}^{-3}$. These are the lowest levels at which total, cardiopulmonary and lung cancer mortality have been shown to increase with more than 95% confidence in response to exposure to $\text{PM}_{2.5}$. The WHO recommends the use of $\text{PM}_{2.5}$ guidelines over PM_{10} because epidemiological studies have shown that most of the adverse health effects associated with PM_{10} are because of $\text{PM}_{2.5}$.

1.2 IDENTIFYING THE SOURCES OF AIRBORNE PARTICLE POLLUTION

Measuring the mass concentration of particulate matter (PM) provides little or no information on the identities of the contributing sources. Airborne particles are composed of many elements and compounds emitted from various sources; and receptor modeling allows the determination of relative mass contributions from sources impacting the total PM mass of samples collected at a monitoring site. Typically, gravimetric mass is measured and then a variety of methods can be used to determine the elements and compounds present in a sample. In this study, elemental concentrations in hourly samples collected in Invercargill were determined using ion beam analysis (IBA) techniques at the New Zealand Ion Beam Analysis facility operated by GNS Science in Lower Hutt. Because a Streaker sampler was used in this study, the hourly PM_{10} mass from a continuous monitor used for compliance monitoring was matched to the hourly elemental concentrations. The Streaker sampler is discussed in more detail in Chapter 2.

Ion beam analysis describes a range of mature analytical techniques that provide the non-destructive determination of multi-elemental concentrations in samples. Using elemental concentrations, coupled with appropriate statistical techniques and purpose-designed mathematical models, the sources contributing to each ambient sample can be identified. In general, the more ambient samples that are included in the analysis, the more robust the receptor modeling results.

Little is known about the PM sources in Invercargill; and nothing is known about how they vary throughout a day. Therefore, this study aimed to identify, using the receptor modeling technique positive matrix factorisation (PMF), the sources contributing to PM concentrations in Invercargill and their mass contributions.

1.3 REPORT STRUCTURE

This report is comprised of 6 main chapters. Briefly, the remaining chapters have been broken down as follows:

1. Chapter 2 describes the methodology and analytical techniques used for the receptor modeling analysis.
2. Chapter 3 describes the Invercargill ambient air quality monitoring site, temporal trends in PM₁₀ concentrations and local meteorology.
3. Chapter 4 presents the receptor modeling results, temporal trends in source contributions, weekday/weekend variations and analyses of source transport.
4. Chapter 5 provides a discussion of the results.
5. Chapter 6 presents recommendations.

2.0 METHODOLOGY

Fine ($PM_{2.5}$) and coarse ($PM_{10-2.5}$) samples were collected using a Streaker sampler at the Environment Southland (ES) monitoring site at Fernworth Primary School on Pomona Street, Invercargill. Figure 2.1 presents the location of the monitoring site.

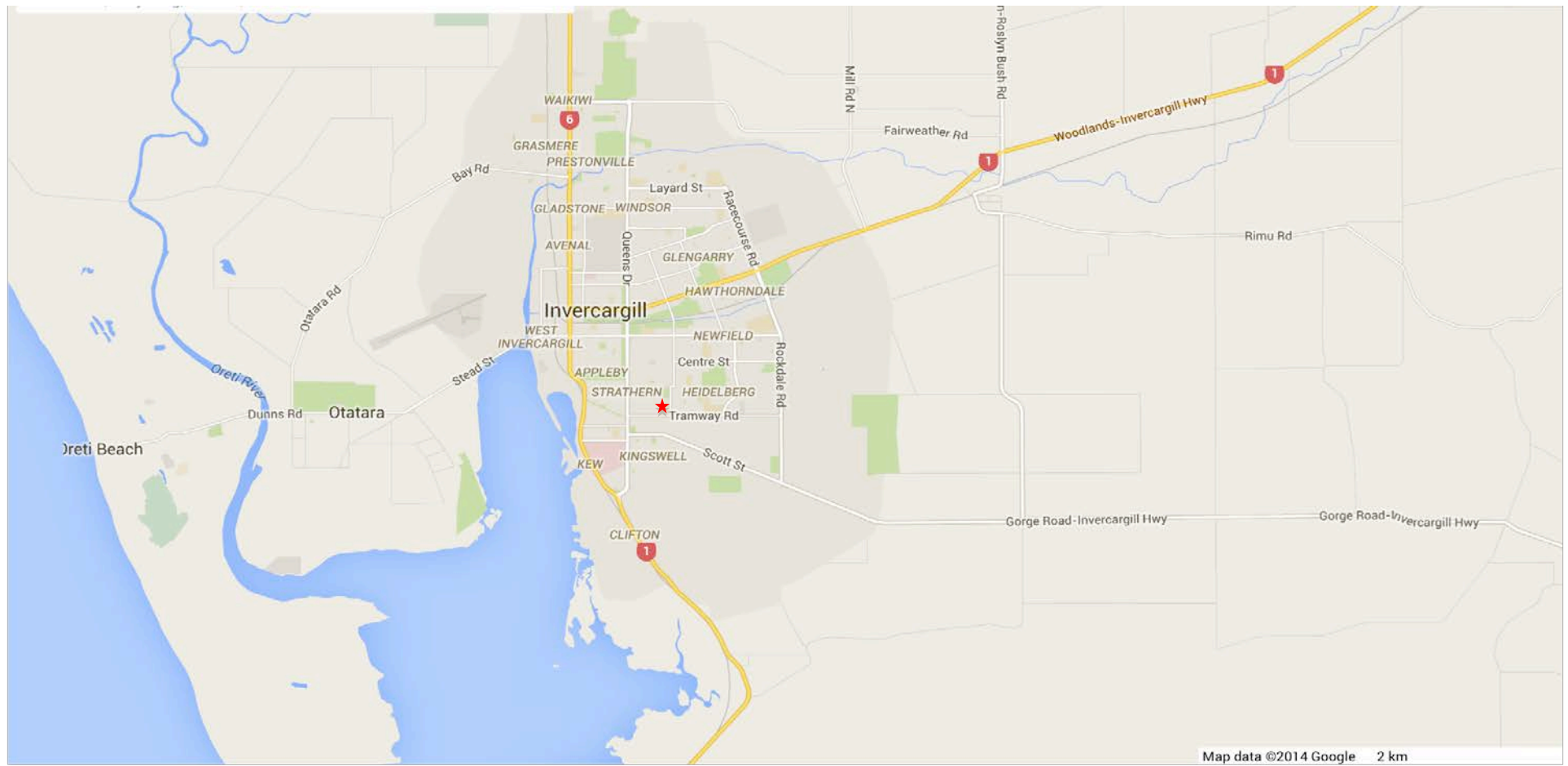


Figure 2.1 Location of the Invercargill monitoring site (★).

The Streaker sampler has previously been described in detail (Annegarn et al., 1988), and used in a number of studies (Ancelet et al., 2012; 2014a; Annegarn et al., 1996). Briefly, the Streaker consists of a pre-impactor that removes particles larger than PM_{10} from the incoming air flow, a thin Kapton foil that collects coarse particles through impaction and a Nucleopore film that collects fine particles. Hourly samples were collected with discrete spacing between each deposit to ensure that each deposit only consisted of PM collected during the intended hour. An image of a typical fine Streaker filter after sampling is presented in Figure 2.2. In this study, 47 samples were collected on each fine and coarse filter.

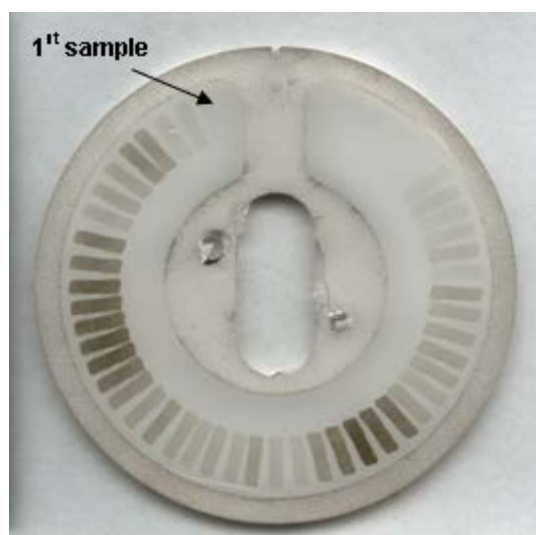


Figure 2.2 Image of a typical fine Streaker filter after sampling. Each spot represents a one hour sample.

Elemental concentrations in the PM_{10} and $PM_{2.5}$ samples were determined using IBA techniques at the New Zealand Ion Beam Analysis Facility in Gracefield, Lower Hutt. The full suite of analyses included particle-induced X-ray emission (PIXE), particle-induced gamma-ray emission (PIGE) and Rutherford backscattering (RBS) analysis. Black carbon (BC) concentrations were determined using light reflection. Full descriptions of the analytical and data analysis techniques used in this study are provided in Appendix 1.

One of the authors (TA) visited the monitoring site and noted typical activities occurring in the surrounding area that may contribute to PM concentrations. These observations are reflected in the conceptual receptor model described in Chapter 3. A meteorological station was also located at the site allowing for investigations into typical meteorological conditions and source transport in the Invercargill airshed.

2.1 DATA ANALYSIS AND REPORTING

The receptor modeling results within this report have been produced in a manner that provides as much information as possible on the relative contributions of sources to PM concentrations so that it may be used for monitoring strategies, air quality management and policy development. The data have been analysed to provide the following outputs:

1. masses of elemental species apportioned to each source;
2. source elemental profiles;
3. average PM₁₀ mass apportioned to each source;
4. temporal variations in source mass contributions;
5. analysis of source contributions on peak PM days. Table 2.1 presents the relevant standards, guidelines and targets for PM concentrations;
6. analysis of the transport of PM from different sources. This includes analyses of meteorological conditions responsible for elevated contributions of the different sources.

Table 2.1 Standards, guidelines and targets for PM concentrations.

Particle Size	Averaging Time	Ambient Air Quality Guideline	MfE* 'Acceptable' air quality category	National Environmental Standard	Allowable Exceedances per Annum
PM ₁₀	24 hours	50 µg m ⁻³	33 µg m ⁻³	50 µg m ⁻³	3 (by 2016)
	Annual	20 µg m ⁻³	13 µg m ⁻³		
PM _{2.5}	24 hours	25 µg m ⁻³	17 µg m ⁻³		

*Ministry for the Environment air quality categories taken from the Ministry for the Environment, October 1997 – *Environmental Performance Indicators: Proposals for Air, Fresh Water and Land*.

3.0 INVERCARGILL MONITORING SITE AND SAMPLING METHODOLOGY

3.1 SITE DESCRIPTION

Size-resolved ($PM_{10-2.5}$ and $PM_{2.5}$) PM samples were collected on an hourly time-scale at an ambient air quality monitoring station operated by Environment Southland on the grounds of Fernworth Primary School (288 Pomona Street; Lat: 46°25'54.16 S, Long: 168°22'14.40, elevation 11 m). Figure 3.1 presents the site location on a map of the local area.

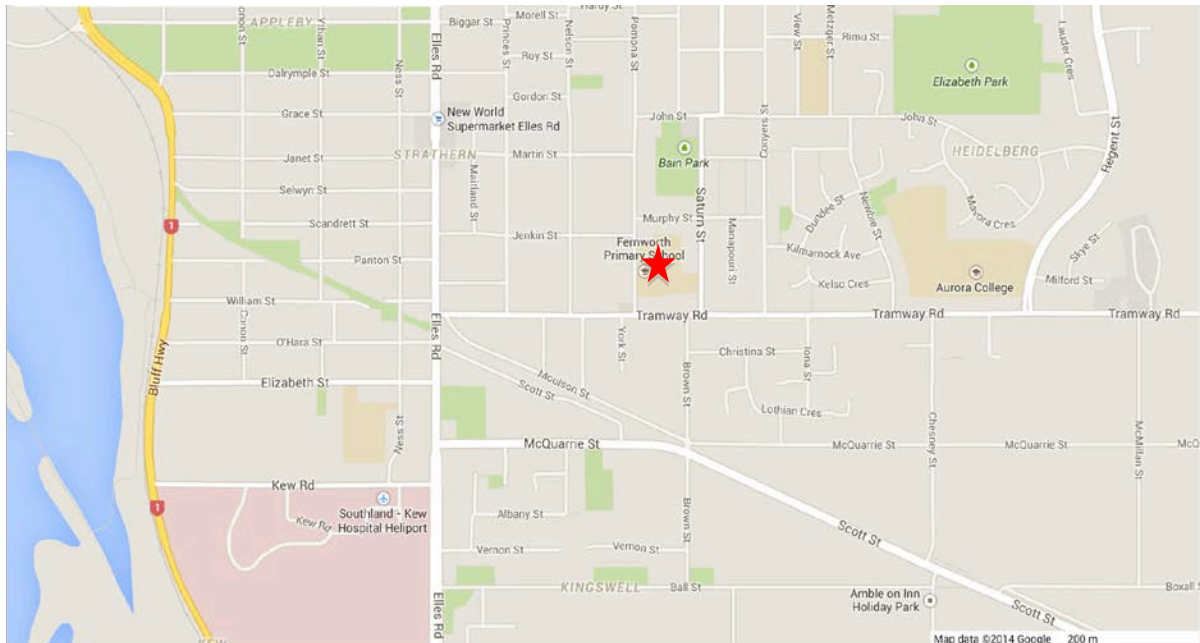


Figure 3.1 Location of the Environment Southland monitoring site at Fernworth Primary School (★).

The Pomona Street monitoring site was located in a field behind Fernworth Primary School and was surrounded by open space or buildings no more than two stories high. The site was approximately 90 m from the nearest road and 2.5 km from the Invercargill CBD. Figure 3.2 presents an aerial photo of the monitoring site and its immediate environs.



Figure 3.2 Aerial photo of the Environment Southland monitoring site and its immediate environs (from Google Earth).

3.2 PARTICULATE MATTER SAMPLING AND MONITORING PERIOD

In this study, fine ($PM_{2.5}$) and coarse ($PM_{10-2.5}$) PM samples were collected on an hourly time-scale using a Streaker sampler (discussed in Chapter 2). The sampler was set to collect samples for 47 hours. Loading of new filters always occurred between 11:00 and 12:00 when PM concentrations tend to be lower than at other times of the day. Overall, 1643 samples of each size fraction were collected (3286 total samples). The hourly PM monitoring campaign ran from 5 June to 22 August 2014.

Because the Streaker sampler collected 47 samples per filter, it was not possible to determine the PM_{10} mass collected gravimetrically. Instead, hourly PM_{10} concentrations were obtained from a co-located FH62 beta-attenuation monitor (BAM) operated by Environment Southland. The fine and coarse samples collected could then be matched to their corresponding PM_{10} concentration for the receptor modeling analysis.

3.3 CONCEPTUAL PM₁₀ RECEPTOR MODEL FOR INVERCARGILL

An important part of the receptor modeling process is to formulate a conceptual model of the receptor site. This means understanding and identifying the major sources that may influence ambient PM concentrations at the site. For the Fernworth Primary School site, the initial conceptual model includes local emission sources:

- Motor vehicles – all roads in the area act as line sources, and roads with higher traffic densities and congestion will dominate;
- Domestic activities – likely to be dominated by biomass burning activities like emissions from solid fuel fires used for domestic heating during the winter;
- Coal combustion in the school's boiler – likely to be most evident when prevailing meteorological conditions direct the plume towards the monitoring site;
- Local wind-blown soil or road dust sources may contribute because there are empty lots and vehicle access ways in close proximity.

Sources that originate further from the monitoring site would also be expected to contribute to ambient particle loadings, and these include:

- Marine aerosol – potentially as separate “fine” and “coarse” sources that have different source regions and temporal variations;
- Secondary PM resulting from atmospheric gas-to-particle conversion processes – includes sulphates, nitrates and organic species;
- Potential industrial emissions from combustion processes (boilers) and dust generating activities, and emissions from the Tiwai Point aluminium smelter.

Another category of emission sources that may contribute are those considered to be ‘one-off’ emission sources:

- Short-term road works and demolition/construction activities.

The variety of sources described above can be recognised and accounted for using appropriate data analysis methods such as examination of seasonal differences, temporal variations and receptor modeling itself.

3.4 LOCAL METEOROLOGY AT THE FERNWORTH PRIMARY SCHOOL SITE

A meteorological station, owned and operated by Environment Southland, was located at the monitoring site. The predominant wind directions at the monitoring site were from the north and southwest, as shown in Figure 3.3. Wind speeds were generally moderate-to-low (< 4 m s⁻¹) during the monitoring period.

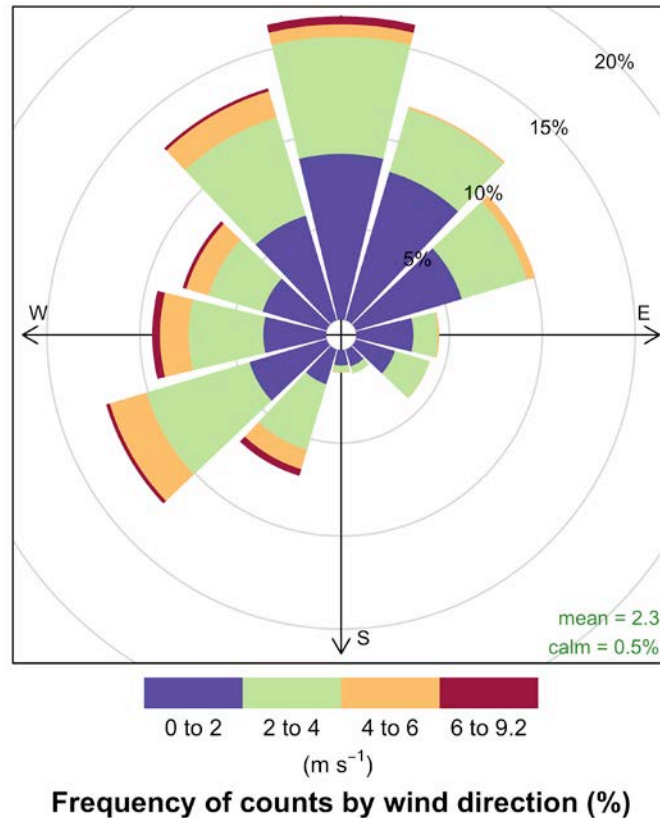


Figure 3.3 Wind rose over the sampling period (June–August 2014).

3.5 PM₁₀ CONCENTRATIONS AT THE FERNWORTH PRIMARY SCHOOL SITE

PM₁₀ concentrations were continuously monitored at the site using a Thermo-Anderson FH62 BAM operated according to AS/NZS 3580.9.11.2008. Figure 3.4 presents the BAM monitoring results, as daily averages (midnight to midnight), from 1 June–31 August 2014. From Figure 3.4 it is apparent that PM₁₀ concentrations exceeded the New Zealand NES (50 µg m⁻³) five times during the sampling period. It should be noted however, that Environment Southland corrects the raw BAM data obtained using a gravimetric equivalent. This means that the actual number of exceedances reported by Environment Southland may differ slightly from the five reported here. Correcting for gravimetric equivalency is a common and reasonable practice for quality assuring data.

Figure 3.5 presents a time series of hourly PM₁₀ concentrations at the monitoring site. It is evident that PM₁₀ concentrations can be highly elevated during certain hours of the day, and these large increases in PM₁₀ concentrations are the main drivers for exceedances of the NES. To understand how PM₁₀ concentrations vary throughout the day, the PM₁₀ diurnal profile was investigated (Figure 3.6). Averaging PM₁₀ concentrations during each hour over the entire sampling period produced the diurnal profile.

Figure 3.6 shows that PM₁₀ concentrations displayed a bimodal diurnal cycle, with concentrations peaking from 18:00–22:00. A smaller peak in concentrations also occurred from 8:00–10:00. This type of pattern is common throughout New Zealand and has previously been identified to be associated with domestic home heating activities (Ancelet et al., 2014a; 2012; 2014b; Trompetter et al., 2010).

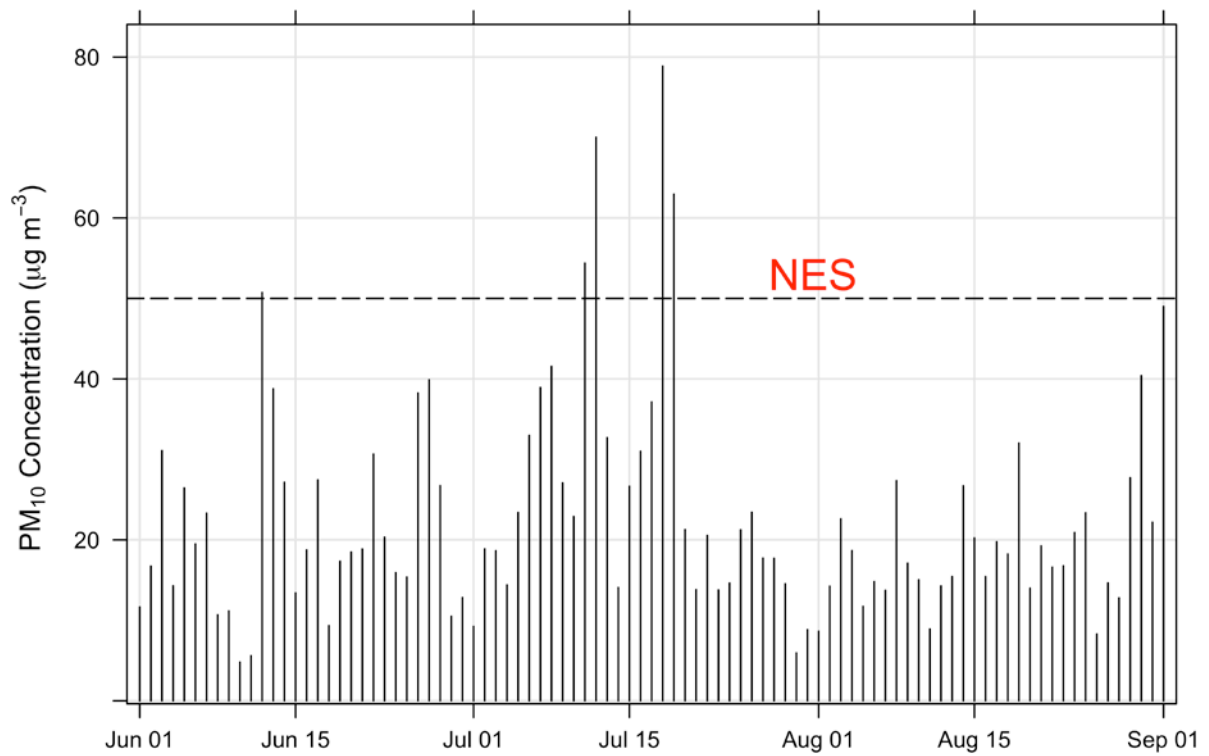


Figure 3.4 Daily PM₁₀ concentrations at Fernworth Primary School. The hashed line indicates the New Zealand National Environmental Standard for PM₁₀ (50 µg m⁻³).

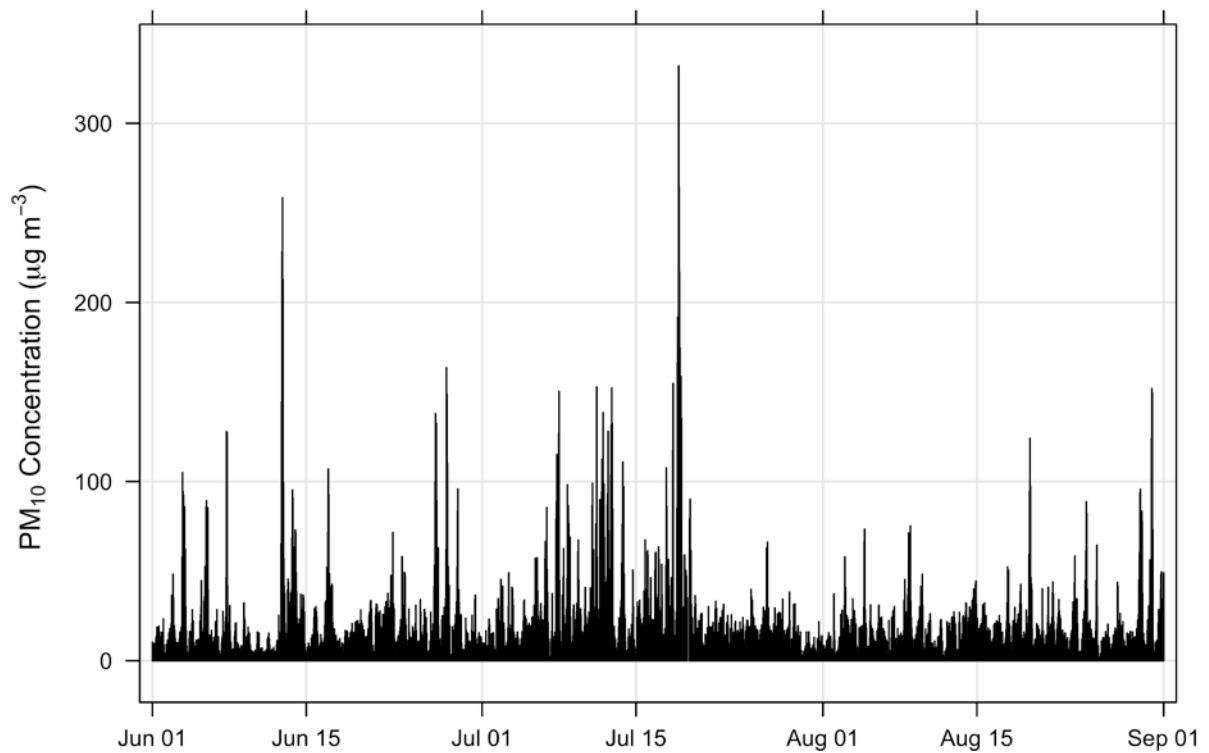


Figure 3.5 Hourly PM₁₀ concentrations at Fernworth Primary School.

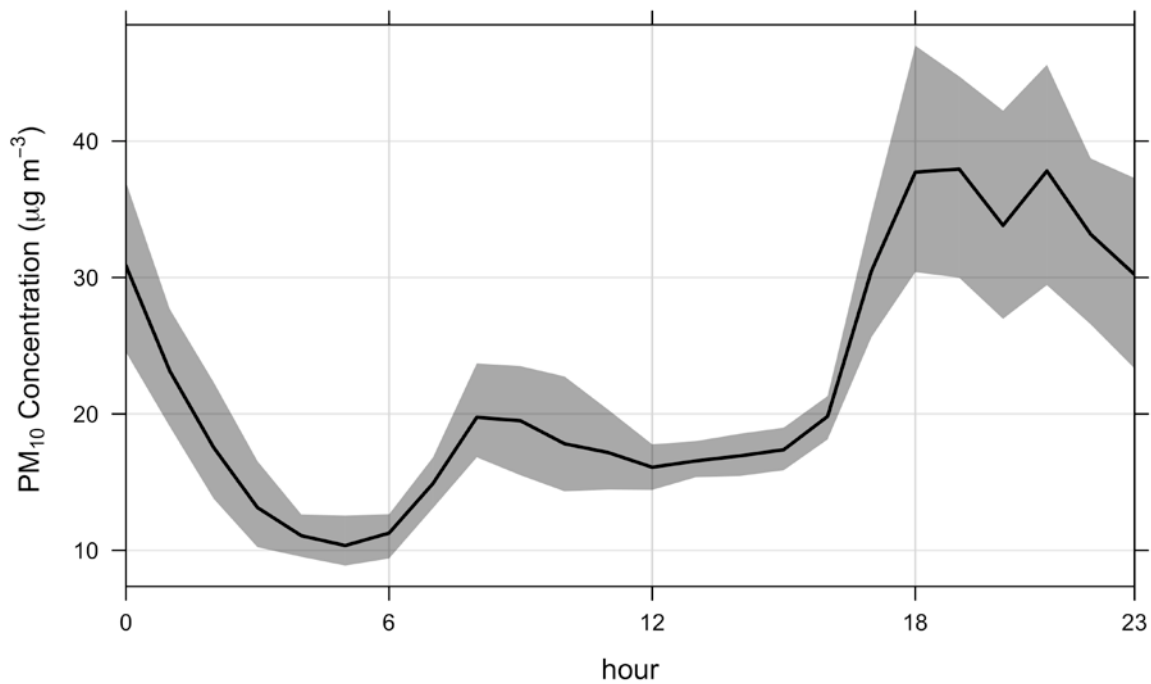


Figure 3.6 Diurnal profile of PM₁₀ concentrations. The solid dark line indicates the average PM₁₀ concentration and the shaded area represents the 95% confidence interval.

Analysing the diurnal profile of PM₁₀ concentrations by day of the week can provide information on potential sources, since vehicular emissions and workplace/industrial emissions would be expected to be lower or show a different profile during weekends. Figure 3.7 presents PM₁₀ diurnal profiles for each day of the week. It is evident from Figure 3.7 that the diurnal profiles do not change dramatically by day of the week, suggesting that the key driver responsible for the measured PM concentrations is not related to workday activities. It is however, interesting that PM₁₀ concentrations tended to be lower from Monday to Wednesday. In fact, to the 95% confidence level, PM₁₀ concentrations on Mondays and Wednesdays were significantly lower than those on Thursdays, Fridays and Saturdays (Figure 3.8). Because the overall diurnal pattern on each of the days was similar, it is likely that meteorological conditions were responsible for the lower concentrations on Mondays and Wednesdays.

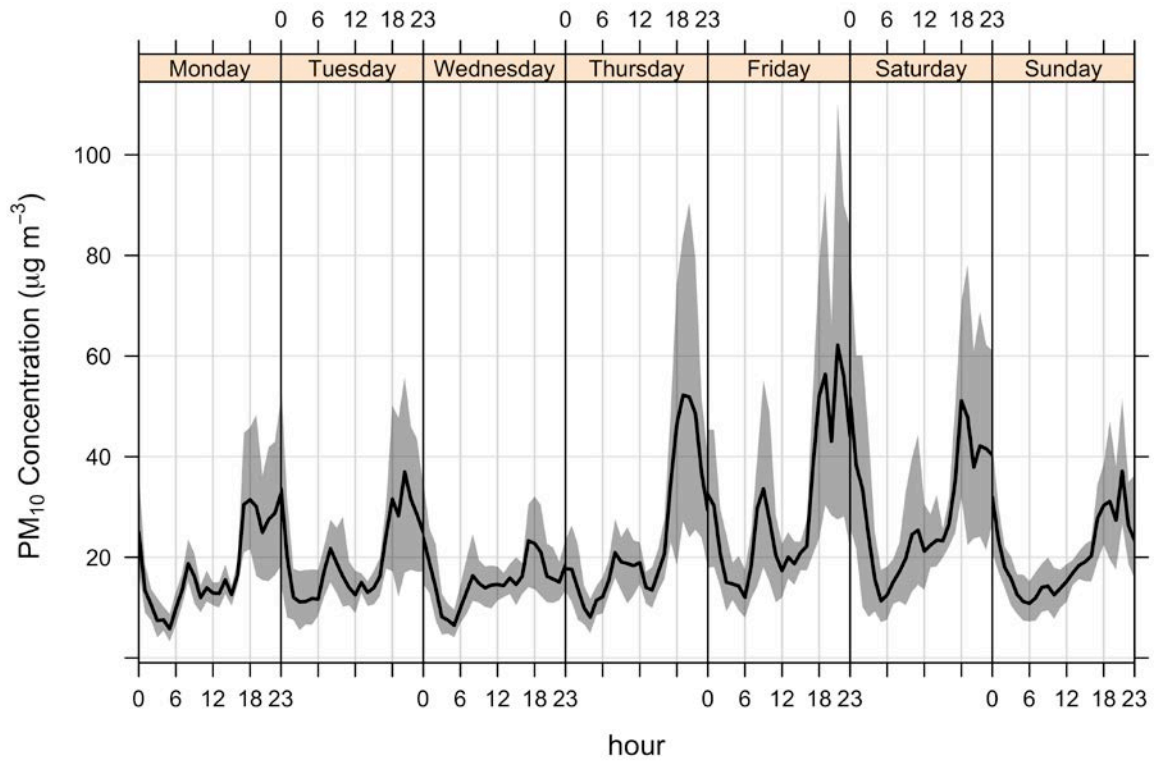


Figure 3.7 Diurnal profiles of PM₁₀ concentrations for each day of the week. The solid dark lines indicate the average PM₁₀ concentration and the shaded areas represent the 95% confidence intervals.

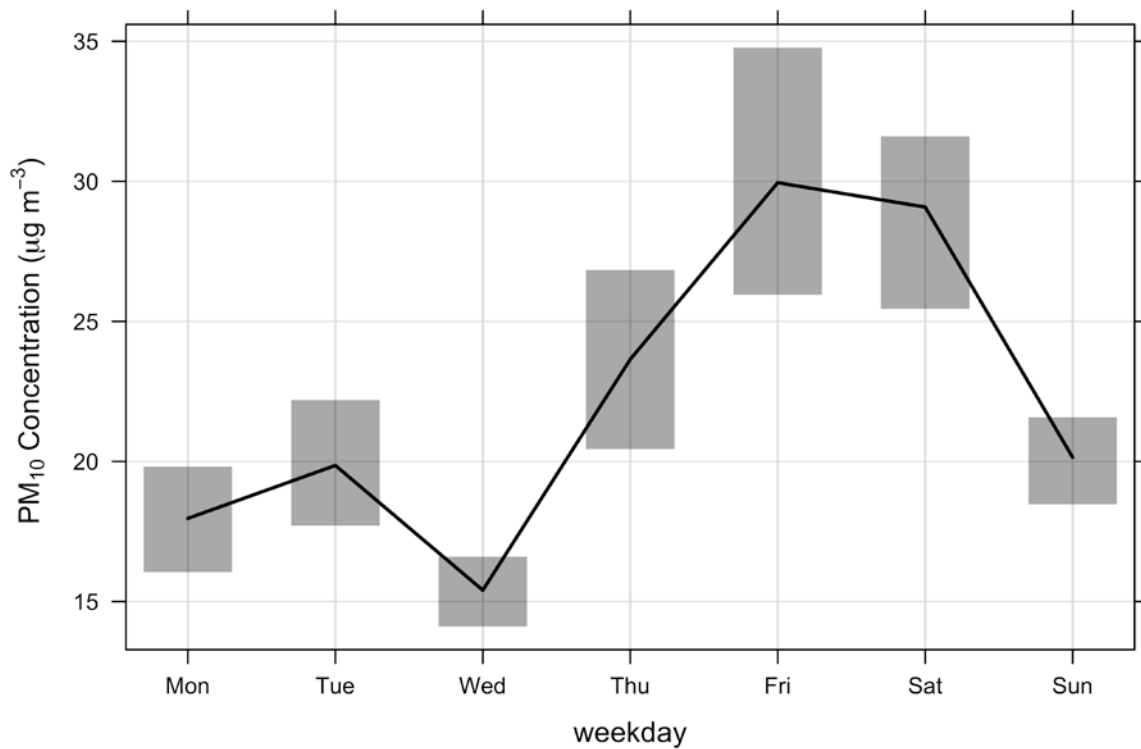


Figure 3.8 Average PM₁₀ concentrations for each day of the week. The solid black line indicates the average concentration and the shaded areas represent the 95% confidence intervals.

To investigate the role that meteorology plays on PM₁₀ concentrations in Invercargill, a bivariate polar plot was produced using the openair package in R (Carlsaw and Ropkins, 2012; R Development Core Team, 2011). Using polar plots to investigate PM₁₀ concentrations is extremely useful because they provide an indication of which wind directions and speeds produce the highest PM₁₀ concentrations. This information is useful for identifying potential sources. Figure 3.9 presents a polar plot of PM₁₀ concentrations. Essentially, Figure 3.9 is a wind rose with PM₁₀ contributions mapped onto it and indicates that peak PM₁₀ concentrations occurred under low wind speeds from the north, with moderate PM₁₀ concentrations occurring under moderate winds from the southwest. In preparing this plot, the weighted mean statistic was used because it combines the concentration data with the frequency of occurrence to identify which wind speeds/directions dominate the overall mean PM₁₀ concentration. Little difference was apparent from polar plots prepared for each day of the week (Figure 3.10).

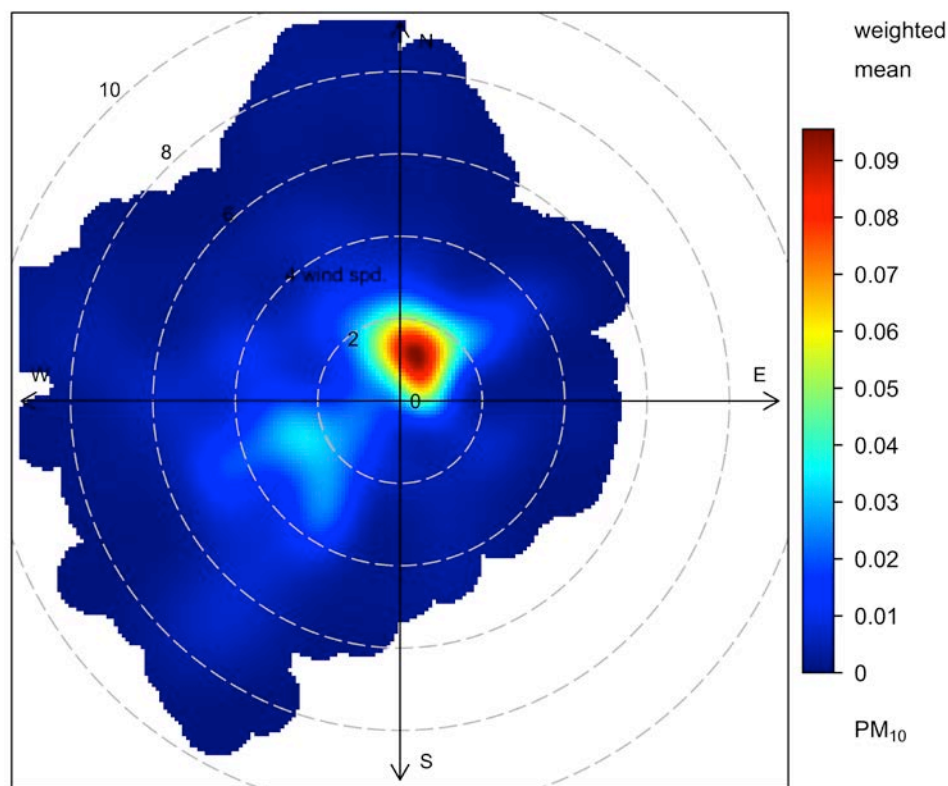


Figure 3.9 Polar plot of PM₁₀ concentrations. The radial dimensions indicate the wind speed in 2 m s⁻¹ increments and the color contours indicate the average contribution to each wind direction/speed bin.

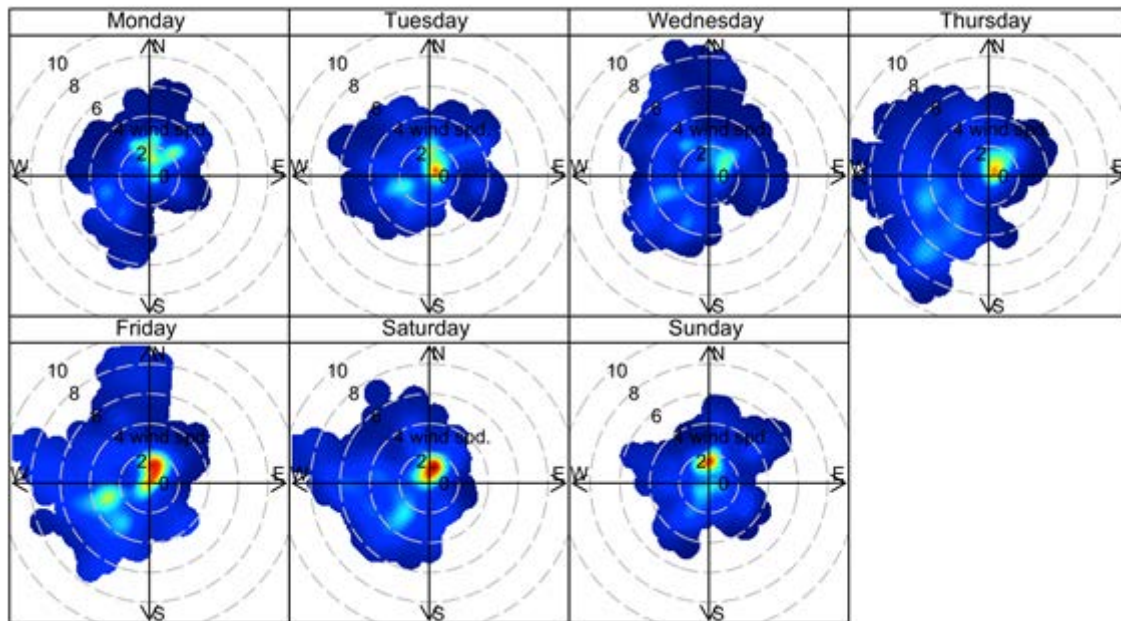


Figure 3.10 Polar plots of PM₁₀ concentrations by day of the week. The radial dimensions indicate the wind speed in 2 m s⁻¹ increments and the color contours indicate the average contribution to each wind direction/speed bin.

This page is intentionally left blank.

4.0 RECEPTOR MODELING ANALYSIS OF PM₁₀ IN INVERCARGILL

4.1 COMPOSITION OF PM_{2.5} AND PM_{10-2.5}

Elemental concentrations for PM_{2.5} and PM_{10-2.5} at Fernworth Primary School are presented in Tables 4.1 and 4.2, respectively. Tables 4.1 and 4.2 indicate that some measured species were close to or below the limits of detection (LOD) in each of the samples. Carbonaceous species, represented by BC, were found to dominate PM_{2.5} mass concentrations. Along with BC, other important elemental constituents included Cl, Si, Fe and S and Na, Cl, S and K in PM_{10-2.5} and PM_{2.5}, respectively, indicating that combustion sources, marine aerosol and soil were important contributors to PM_{10-2.5} and PM_{2.5} at the monitoring site. An elemental correlation plot is provided as Figure A2.1 in Appendix 2. The filters, used as received from PIXE International (Tallahassee, USA), were contaminated with Al, Si and Ca. This was particularly true for the fine filters. As such, Si and Al results from the fine filters could not be used in the receptor modeling.

Table 4.1 Elemental concentrations in PM_{2.5} collected at Fernworth Primary School (1643 samples).

	Average (ng m ⁻³)	Max (ng m ⁻³)	Min (ng m ⁻³)	Median (ng m ⁻³)	StdDev (ng m ⁻³)	Ave Uncert (ng m ⁻³)	Ave LOD (ng m ⁻³)	#>LOD	%>LOD
BC	4117	20429	139	3662	3127	502	800	1409	86
Na	622	2392	0	672	412	303	1334	53	3
Mg	90	269	0	88	59	80	123	533	32
Al	15	1023	0	0	53	68	89	82	5
Si	956	2496	318	942	182	44	44	1643	100
P	5	78	0	0	10	41	52	56	3
S	184	1510	22	143	135	21	28	1641	100
Cl	250	2183	0	136	299	23	28	1555	95
K	126	1502	0	79	152	19	27	1415	86
Ca	41	294	0	37	26	17	24	1255	76
Sc	6	46	0	2	7	19	27	81	5
Ti	3	32	0	0	5	19	25	30	2
V	3	30	0	0	5	14	19	88	5
Cr	6	33	0	5	6	10	13	382	23
Mn	3	26	0	0	4	10	12	243	15
Fe	22	372	0	14	28	7	9	1200	73
Co	3	23	0	0	4	9	12	124	8
Ni	2	33	0	0	3	8	11	79	5
Cu	5	508	0	0	24	10	13	123	7
Zn	13	473	0	6	29	13	17	359	22
Ga	2	24	0	0	4	15	18	6	0
Ge	2	37	0	0	5	22	27	6	0
As	5	144	0	0	13	29	34	43	3
Se	4	132	0	0	10	31	37	11	1
Br	46	233	0	43	41	53	70	527	32
Rb	7	136	0	0	18	79	96	4	0
Sr	8	210	0	0	23	82	99	3	0
Mo	18	390	0	0	54	224	268	1	0
I	21	219	0	3	30	69	90	88	5
Ba	11	124	0	0	18	56	77	29	2
Hg	14	288	0	0	23	55	67	10	1
Pb	7	320	0	0	23	89	98	9	1

Table 4.2 Elemental concentrations in PM_{10-2.5} collected at Fernworth Primary School (1643 samples).

	Average (ng m ⁻³)	Max (ng m ⁻³)	Min (ng m ⁻³)	Median (ng m ⁻³)	StdDev (ng m ⁻³)	Ave Uncert (ng m ⁻³)	Ave LOD (ng m ⁻³)	#>LOD	%>LOD
Na	1022	6648	0	944	814	360	1334	402	24
Mg	112	445	0	106	71	84	128	679	41
Al	40	251	0	34	38	53	78	415	25
Si	35	418	0	9	52	33	46	475	29
P	12	96	0	5	15	36	49	149	9
S	35	489	0	27	37	24	37	701	43
Cl	471	4697	0	70	747	32	35	1101	67
K	48	370	0	38	45	22	33	949	58
Ca	30	436	0	18	39	22	28	641	39
Sc	8	56	0	4	9	22	33	86	5
Ti	4	392	0	0	12	22	29	59	4
V	4	41	0	0	6	17	23	80	5
Cr	6	36	0	4	7	14	18	253	15
Mn	4	37	0	0	5	12	16	196	12
Fe	21	486	0	16	25	8	11	1180	72
Co	3	35	0	0	4	11	14	165	10
Ni	3	43	0	0	4	10	13	150	9
Cu	5	468	0	0	15	11	15	168	10
Zn	6	271	0	0	14	13	17	142	9
Ga	2	28	0	0	5	15	19	14	1
Ge	2	41	0	0	5	21	26	11	1
As	2	68	0	0	6	29	34	6	0
Se	4	94	0	0	10	32	39	11	1
Br	5	119	0	0	12	45	54	9	1
Rb	7	115	0	0	18	69	83	3	0
Sr	9	139	0	0	23	87	105	4	0
Mo	28	371	0	0	70	239	287	1	0
I	14	194	0	0	29	92	115	45	3
Ba	12	128	0	0	20	67	93	20	1
Hg	7	93	0	0	16	57	70	2	0
Pb	6	121	0	0	17	79	85	1	0

4.2 SOURCE CONTRIBUTIONS TO PM₁₀

Five source contributors were identified from PMF receptor modeling analysis of the elemental data. Figure 4.1 presents the source profiles extracted from the PMF analysis. The source contributors identified in Figure 4.1 were found to explain 84% of the PM₁₀ mass. The sources identified were:

- The first factor was identified as biomass combustion based on the presence of BC and K as primary species, along with some Cl and S. Interestingly arsenic and lead were strongly associated with the biomass combustion profile, suggesting that residents are burning copper chrome arsenate (CCA)-treated and lead painted timber in their domestic solid fuel heaters.
- The second factor was identified as coarse marine aerosol because of the predominance of PM_{10-2.5} Cl, along with some S, K and Ca.
- The third factor was identified as crustal matter, or soil, and featured Si, S, K, Ca and Fe as the primary species.
- The fourth factor was termed fine marine aerosol based on the dominance of PM_{2.5} Cl, along with some S, K and Ca. This factor is distinct from the coarse marine aerosol factor because it likely results from longer-range transport and shows a different temporal variation (discussed in Chapter 4.3).
- The fifth factor was identified as originating from motor vehicle emissions because of the presence of BC, S, Si, Ca and Fe as significant components representing a combination of tailpipe emissions and re-entrained road dust. Copper present in the profile also indicates emissions from the wear of brake linings.

The average PM₁₀ source contributions estimated by PMF (Figure 4.2) indicated that biomass combustion was the dominant contributor to PM₁₀ mass (68%). Marine aerosol (fine and coarse, 21%) and motor vehicles (10%) had smaller contributions to PM₁₀ mass, while crustal matter (1%) had little impact at the monitoring site. Because this study was performed during the winter, it is not surprising that biomass combustion was the largest source contributor because many homes in Invercargill use solid fuel fires for domestic heating. The relatively low contributions of coarse marine aerosol and crustal matter are likely related to the lower wind speeds typically experienced during winter.

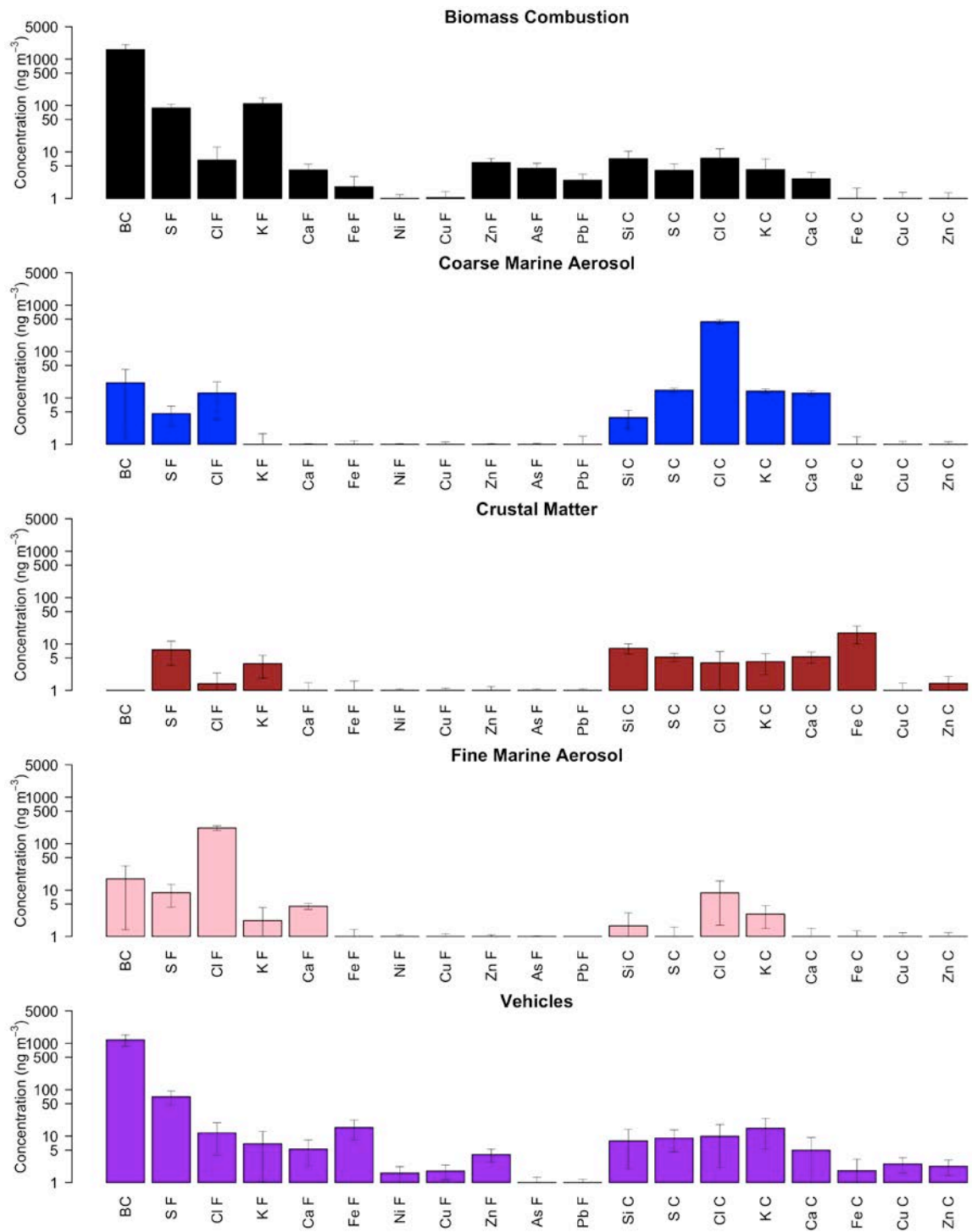


Figure 4.1 PM₁₀ source profiles at Fernworth Primary School.

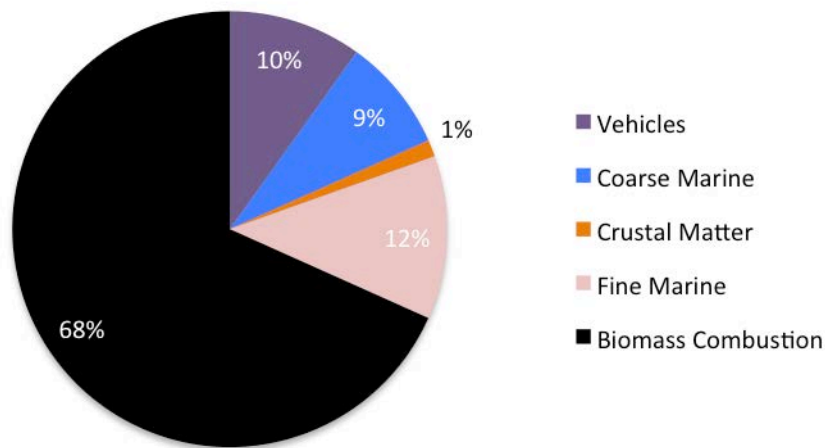


Figure 4.2 Average source contributions to PM₁₀ at Fernworth Primary School.

4.3 TEMPORAL VARIATIONS IN SOURCE CONTRIBUTIONS

Temporal variations in the PM₁₀ source contributions are presented in Figure 4.3. Gaps present in Figure 4.3 are from missed sampling days. It is evident from Figure 4.3 that each source has distinct diurnal cycles and that, at times, marine aerosol contributions can be significant. It is also clear that fine and coarse marine aerosol are distinct sources because their temporal variations can differ substantially.

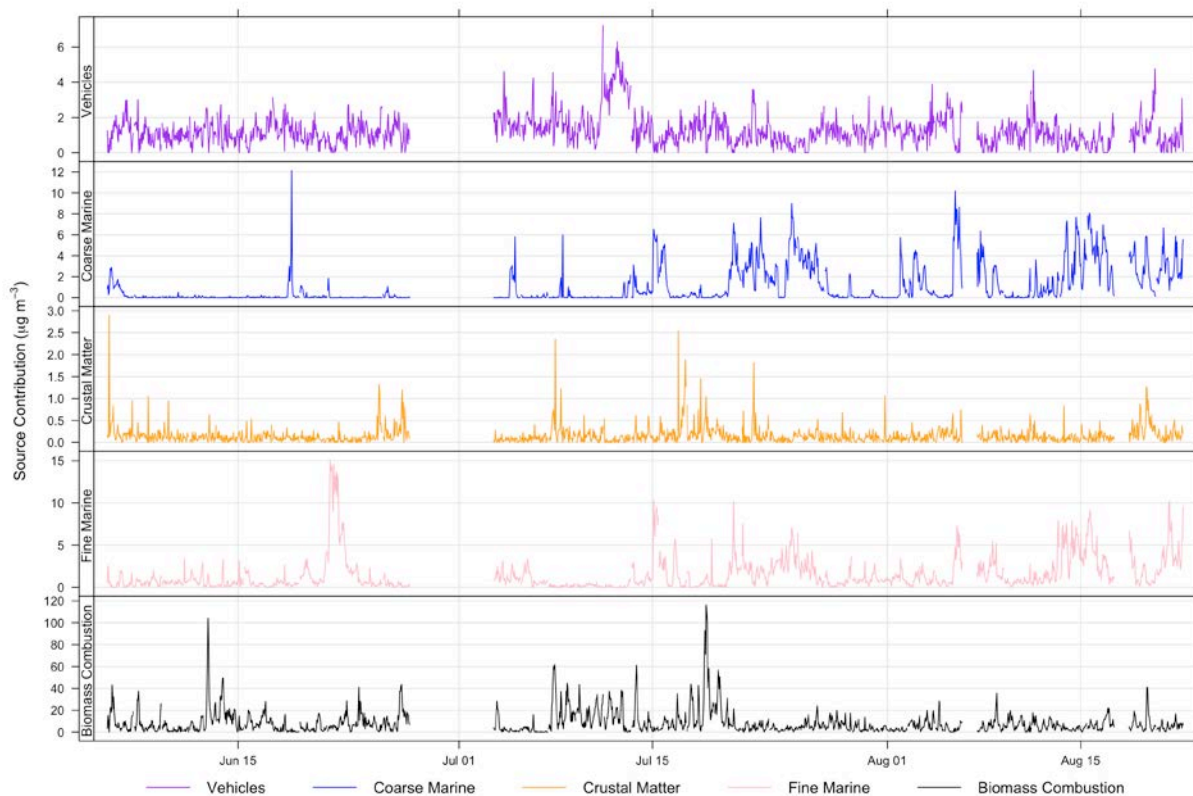


Figure 4.3 Temporal variations in source contributions to PM₁₀ at Fernworth Primary School. Gaps in the data are from missed sampling days.

To further investigate how the different source contributors varied throughout a day, the average hourly diurnal contribution profiles for each source were evaluated. Figure 4.4 presents the average hourly diurnal profile for biomass combustion. Biomass combustion had a bimodal diurnal profile, with a large peak in contributions from 18:00–21:00 and a smaller peak from 7:00–9:00. This suggests that residents are re-lighting their fires when they rise in the morning. This result is similar to other locations throughout New Zealand (Ancelet et al., 2014b; 2014a; 2012). Because biomass combustion was the dominant source, its diurnal profile closely matches that of PM₁₀ (Figure 3.6).

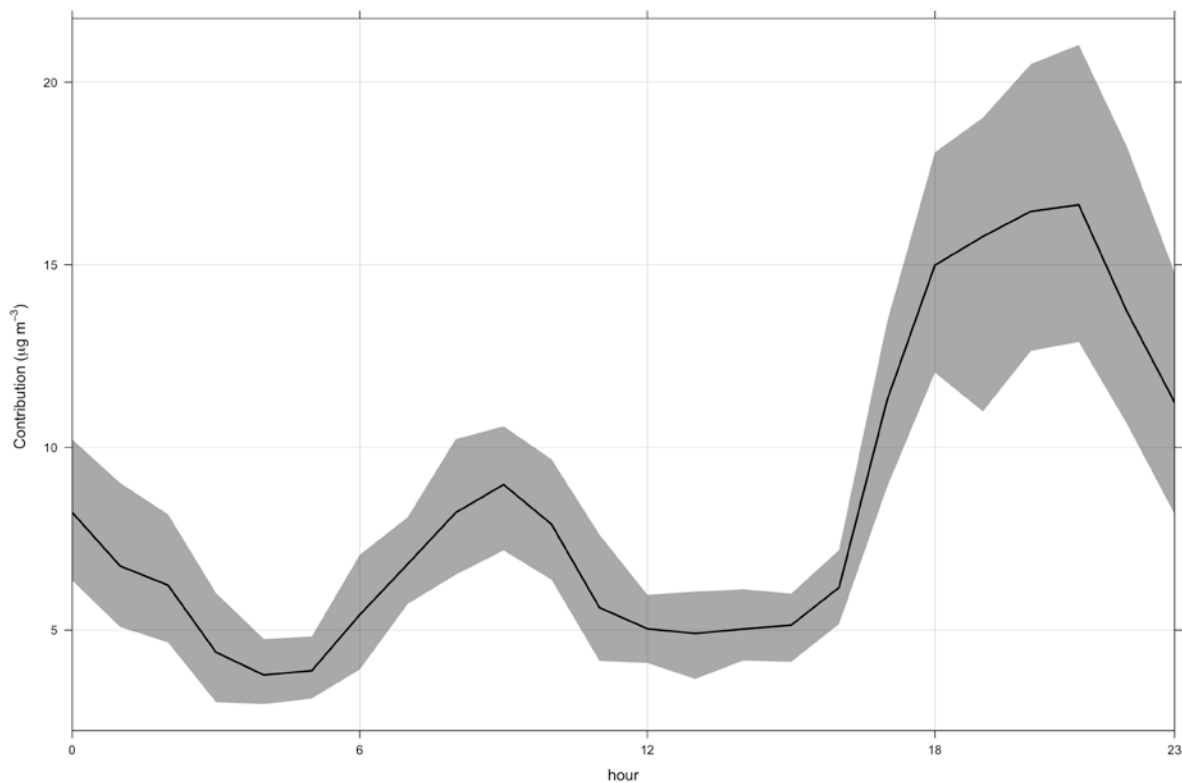


Figure 4.4 Average hourly diurnal profile of the biomass combustion source. The solid black line indicates the average concentration ($\mu\text{g m}^{-3}$) and the shaded area represents the 95% confidence intervals.

The average hourly diurnal profile for the motor vehicle source, presented in Figure 4.5, is markedly different from that of biomass combustion. Figure 4.5 shows that motor vehicle contributions peaked during the morning rush hour (7:00–10:00), decreased slightly over the day, and then peaked again during the evening rush hour (16:00–17:00). This type of diurnal pattern is expected given the nature of vehicle use.

Crustal matter contributions (Figure 4.6) peaked during the morning and afternoon-evening. Typically crustal matter contributions increase under elevated wind speeds, but can also be related to anthropogenic activities occurring near the monitoring site. Chapters 4.4 and 4.5 present further analyses to identify whether the crustal matter source is simply a natural source contributor, or was influenced by anthropogenic activities near the monitoring site.

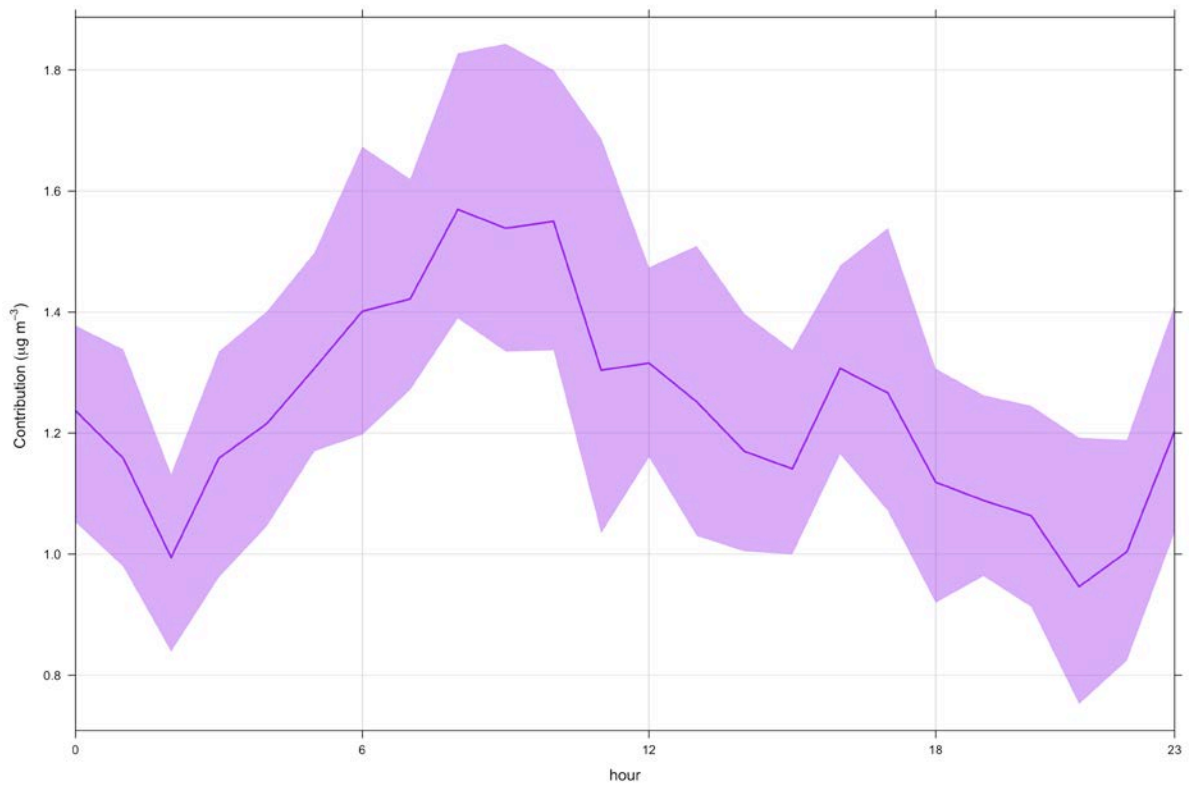


Figure 4.5 Average hourly diurnal profile of the motor vehicle source. The solid purple line indicates the average concentration ($\mu\text{g m}^{-3}$) and the shaded area represents the 95% confidence intervals.

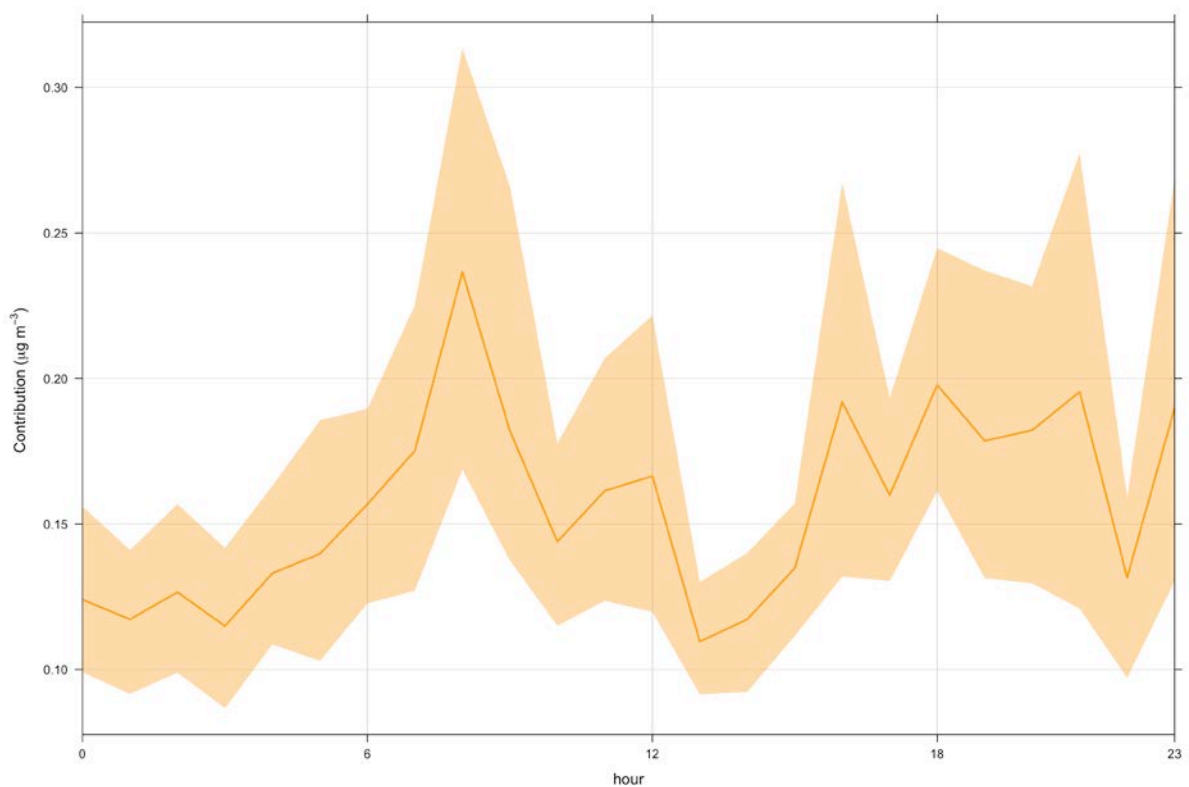


Figure 4.6 Average hourly diurnal profile of the crustal matter source. The solid orange line indicates the average concentration ($\mu\text{g m}^{-3}$) and the shaded area represents the 95% confidence intervals.

Figures 4.7 and 4.8 present the average hourly diurnal profiles of coarse and fine marine aerosol, respectively. Both sources showed little variation throughout the day, but did tend to increase in the afternoon when wind speeds are typically higher.

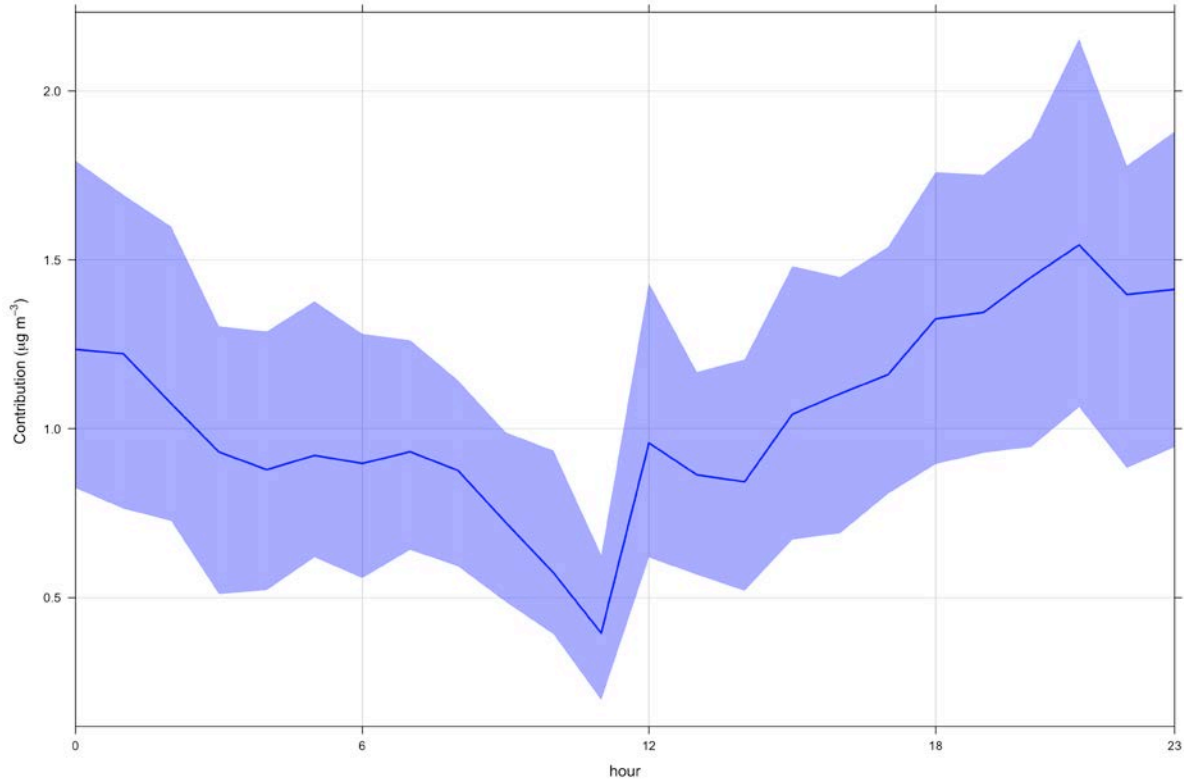


Figure 4.7 Average hourly diurnal profile of the coarse marine aerosol source. The solid blue line indicates the average concentration ($\mu\text{g m}^{-3}$) and the shaded area represents the 95% confidence intervals.

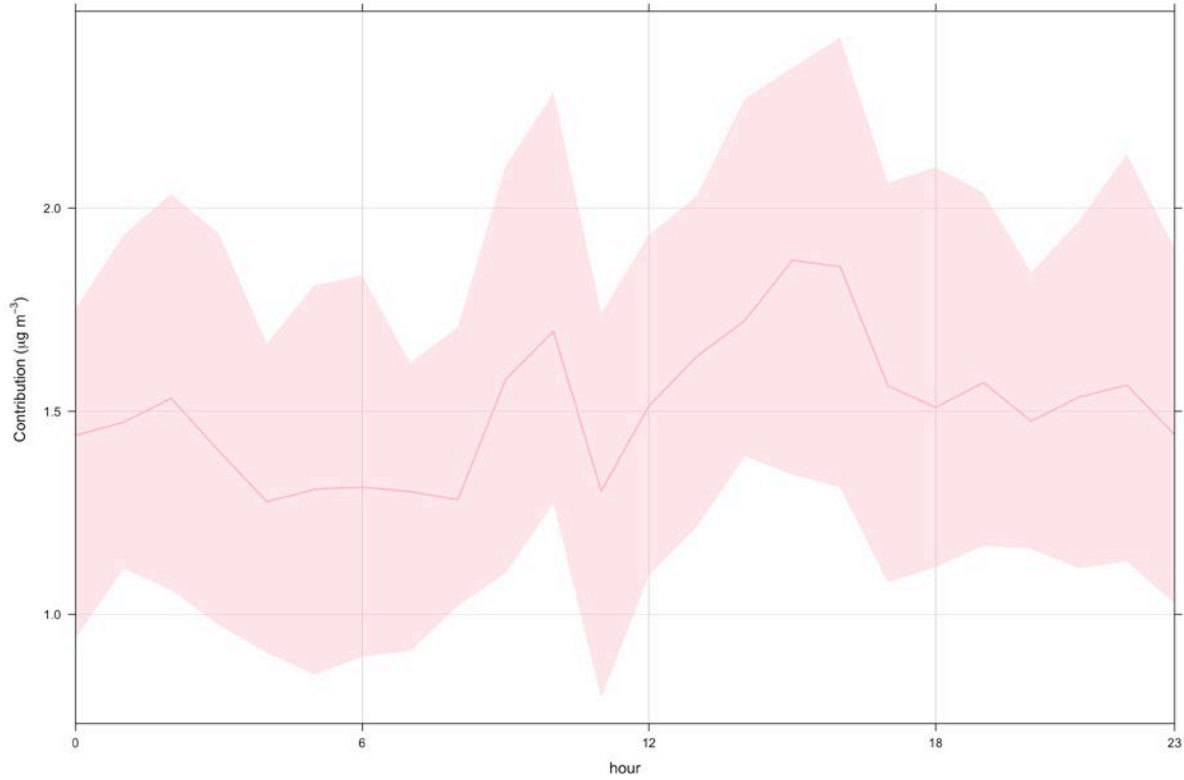


Figure 4.8 Average hourly diurnal profile of the fine marine aerosol source. The solid pink line indicates the average concentration ($\mu\text{g m}^{-3}$) and the shaded area represents the 95% confidence intervals.

Overall, combining the hourly contributions for each source provides a visualisation of how much each source contributes to measured PM₁₀ concentrations throughout a day. Figure 4.9 presents a plot of average hourly source contributions for each of the sources. From Figure 4.9 it is clear that biomass combustion is the dominant contributor during all hours of the day.

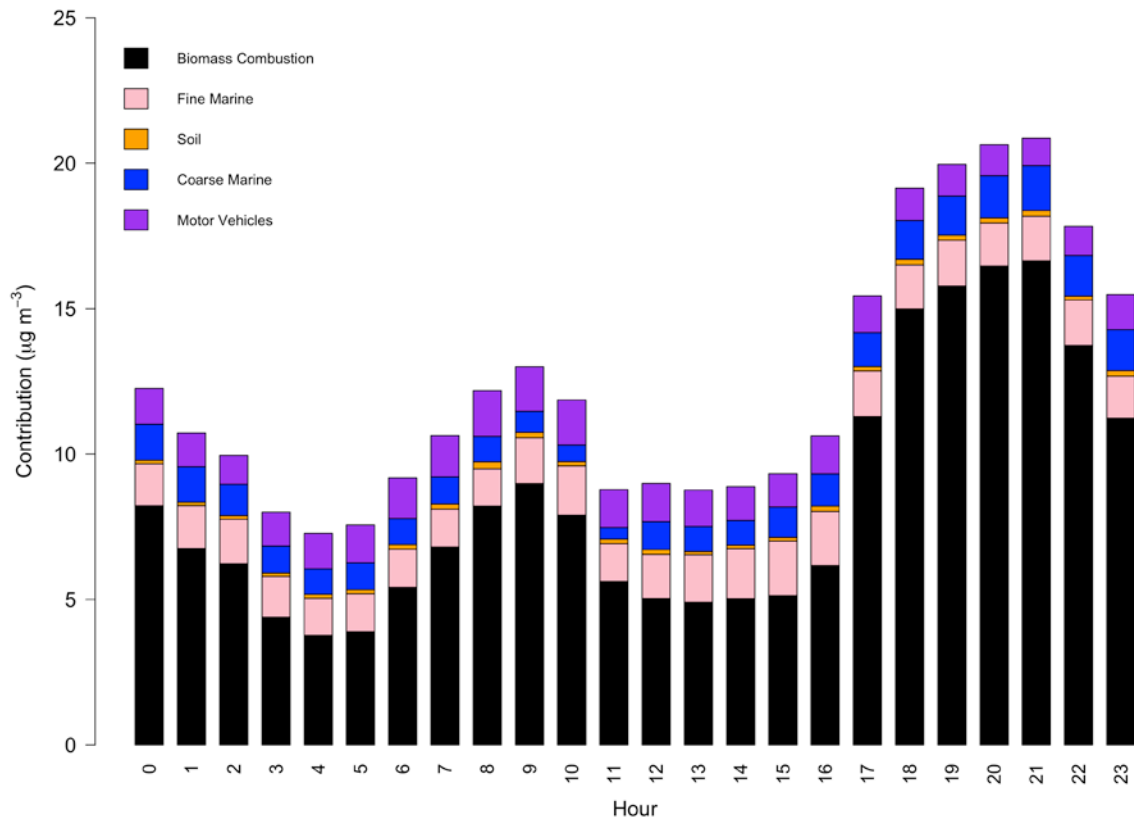


Figure 4.9 Average hourly source contributions ($\mu\text{g m}^{-3}$) at Fernworth Primary School.

4.4 WEEKDAY/WEEKEND VARIATIONS IN SOURCE CONTRIBUTIONS

To evaluate how source contributions varied by day of the week, average source contributions for each day were evaluated. This type of analysis can provide important information because it can indicate whether a potentially natural source (e.g., crustal matter) may be influenced by anthropogenic activities. Figure 4.10 presents biomass combustion contributions by day of the week. At the 95% confidence level biomass combustion contributions did not show much variation throughout the week, although biomass combustion contributions were lowest on Wednesdays and increased from Thursday to Saturday. Because biomass combustion contributions tend to increase under calm meteorological conditions, it would not be expected to observe a distinct weekday/weekend variation in its contributions unless there are strong behavioural reasons for increased wood burning on Thursdays, Fridays and Saturdays.

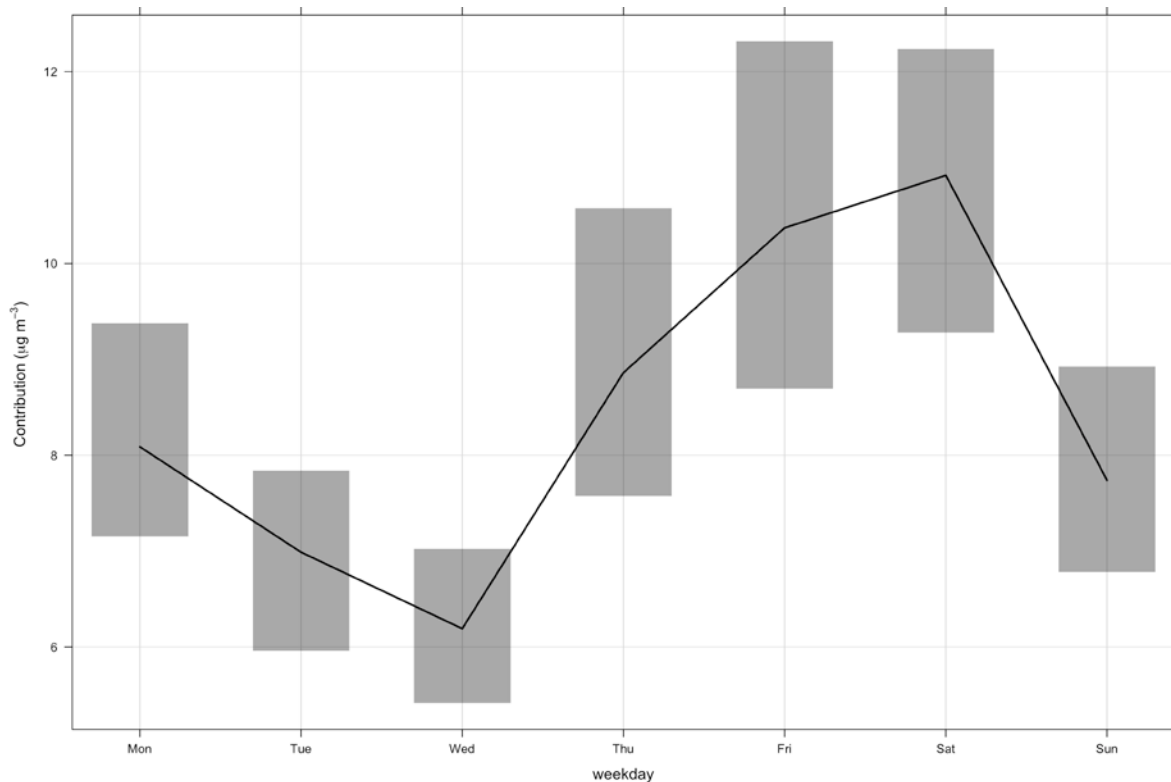


Figure 4.10 Biomass combustion contributions ($\mu\text{g m}^{-3}$) by day of the week. The solid black line indicates the average contribution and the shaded areas represent the 95% confidence intervals.

The motor vehicle source also showed little variation between weekdays and weekends (Figure 4.11). While it would be expected that motor vehicle contributions during weekdays would be higher, it is possible that the more residential nature of the monitoring site, as opposed to being located in the city center, played a role in the observed weekday/weekend pattern. In fact, motor vehicle contributions on Saturdays were significantly higher than those on Wednesdays and Thursdays. It is also possible that local meteorology influenced peak motor vehicle contributions.

Crustal matter contributions (Figure 4.12) showed a different weekday/weekend variation than biomass combustion and motor vehicles. Crustal matter contributions were lower, sometimes significantly, on Saturdays and were significantly lower on Sundays than all other days. The higher weekday contribution from crustal matter in PM_{10} suggests that re-entrainment by motor vehicles and/or local activities such as construction or school activities could have an important influence on crustal matter contributions.

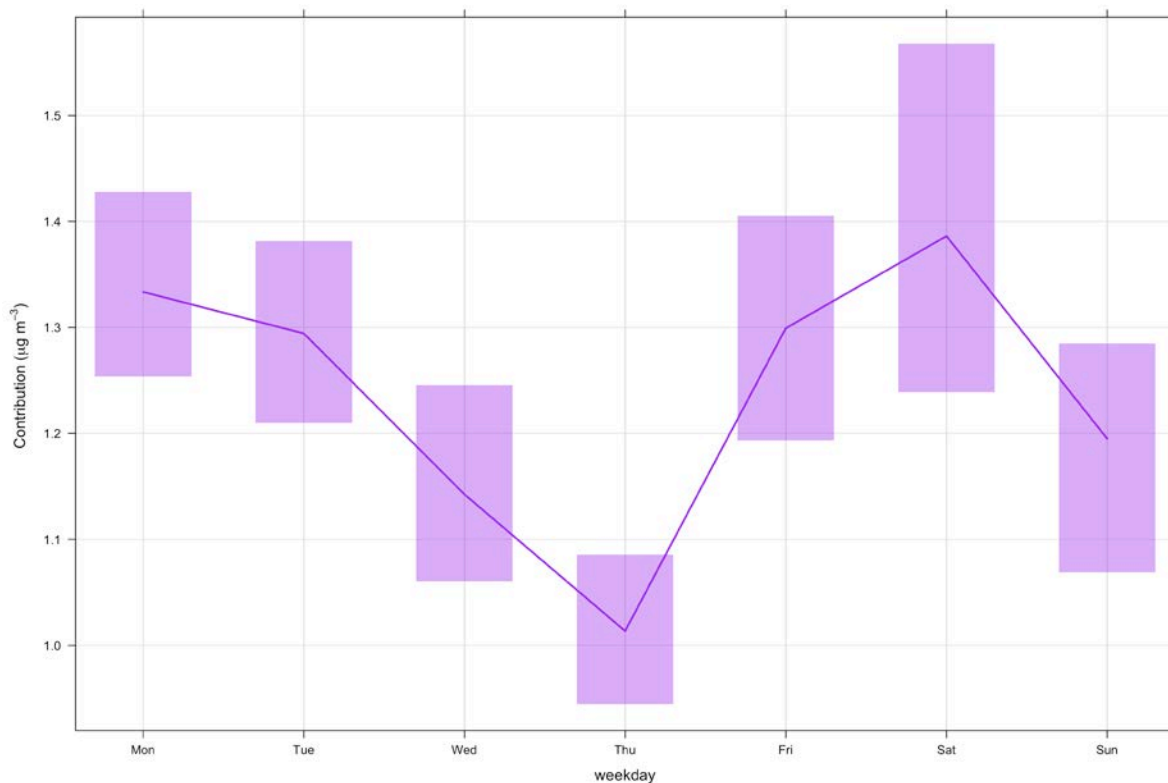


Figure 4.11 Motor vehicle contributions ($\mu\text{g m}^{-3}$) by day of the week. The solid purple line indicates the average contribution and the shaded areas represent the 95% confidence intervals.

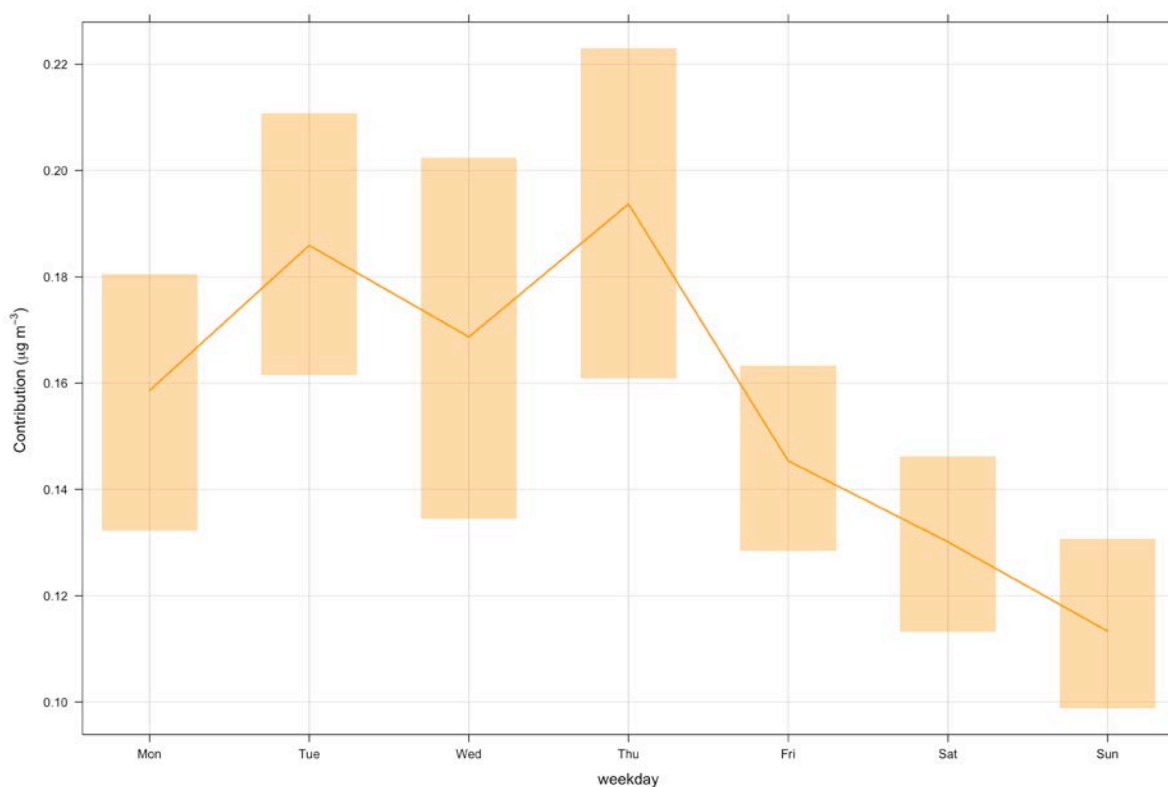


Figure 4.12 Crustal matter contributions ($\mu\text{g m}^{-3}$) by day of the week. The solid orange line indicates the average contribution and the shaded areas represent the 95% confidence intervals.

Coarse and fine marine aerosol (Figures 4.13 and 4.14, respectively) showed little weekday/ weekend variation because they are both natural sources influenced only by meteorological conditions.

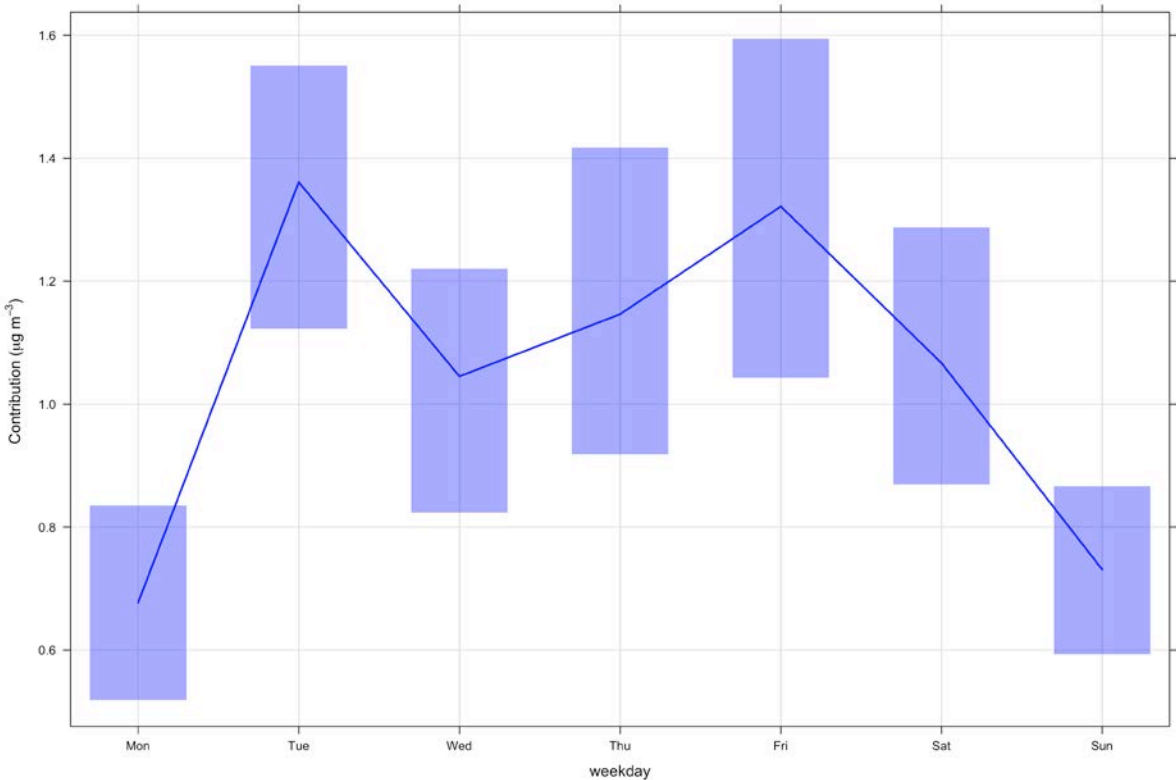


Figure 4.13 Coarse marine aerosol contributions ($\mu\text{g m}^{-3}$) by day of the week. The solid blue line indicates the average contribution and the shaded areas represent the 95% confidence intervals.

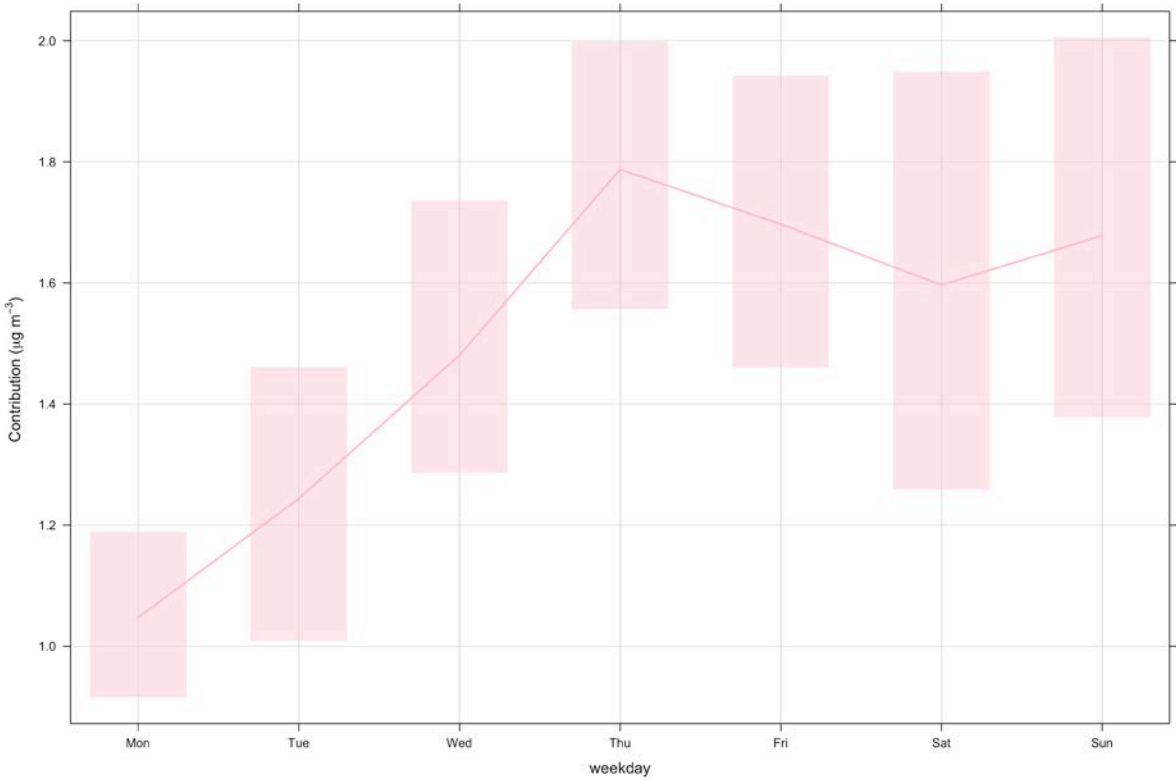


Figure 4.14 Fine marine aerosol contributions ($\mu\text{g m}^{-3}$) by day of the week. The solid pink line indicates the average contribution and the shaded areas represent the 95% confidence intervals.

4.5 VARIATIONS IN SOURCE CONTRIBUTIONS WITH WIND DIRECTION

Bivariate polar plots, discussed in Chapter 3.5, were used to evaluate how wind speed and direction affect contributions from the different sources. These plots can also provide important information about how pollutant concentrations build up at a particular site.

4.5.1 Biomass combustion

Biomass combustion source contributions to PM_{10} and are considered to be primarily from domestic solid fuel fire emissions. Figure 4.15 presents a bivariate polar plot of biomass combustion contributions to PM_{10} . Figure 4.15 shows that peak biomass combustion contributions occurred under low wind speeds ($< 2 \text{ m s}^{-1}$) from the north. This indicates that katabatic flows under cold and calm anticyclonic synoptic meteorological conditions coupled with domestic fire emissions and poor dispersion were responsible for elevated biomass combustion contributions, similar to previous results in other New Zealand locations (Ancelet et al., 2014b; 2014a; 2012). Such meteorological conditions can reasonably be anticipated one or two days ahead of time so that it can be used as a predictor of high concentrations of particulate matter pollution due to domestic fires or to issue warnings of an air pollution risk.

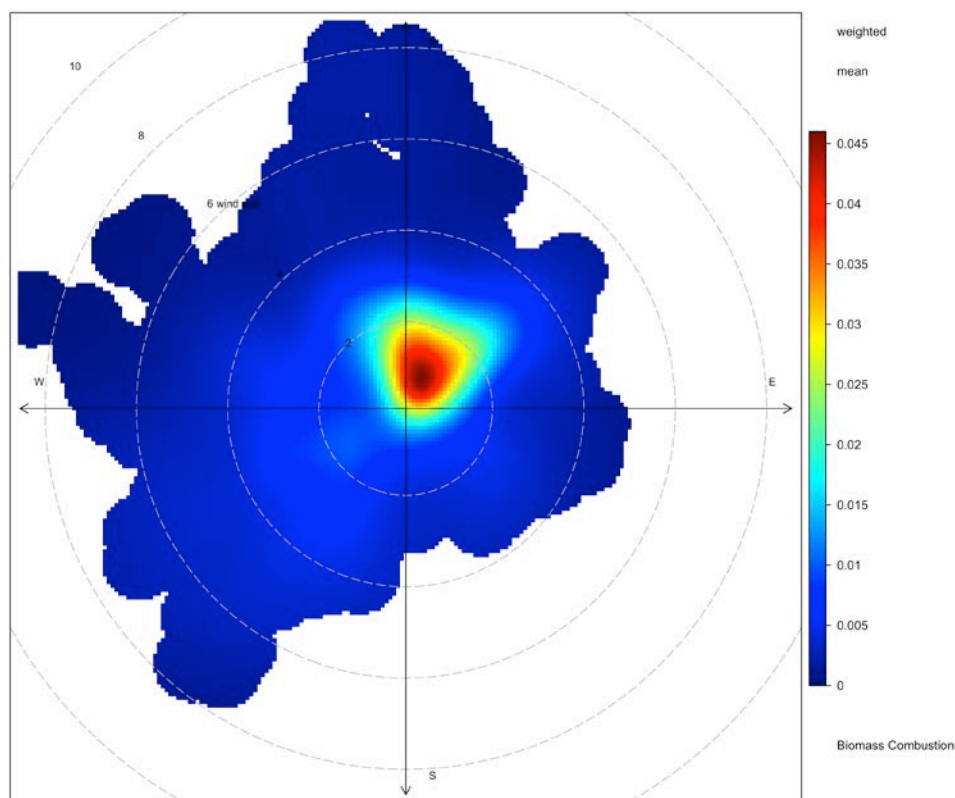


Figure 4.15 Polar plot of biomass combustion contributions. The radial dimensions indicate the wind speed in 2 m s^{-1} increments and the color contours indicate the average contribution to each wind direction/speed bin.

4.5.2 Motor vehicles

The motor vehicle source showed a north-northwest directionality, peaking under moderate wind speeds from the north (Figure 4.16). This source was likely influenced both by the common northerly winds in Invercargill and the fact that the more trafficked CBD area was north of the monitoring site.

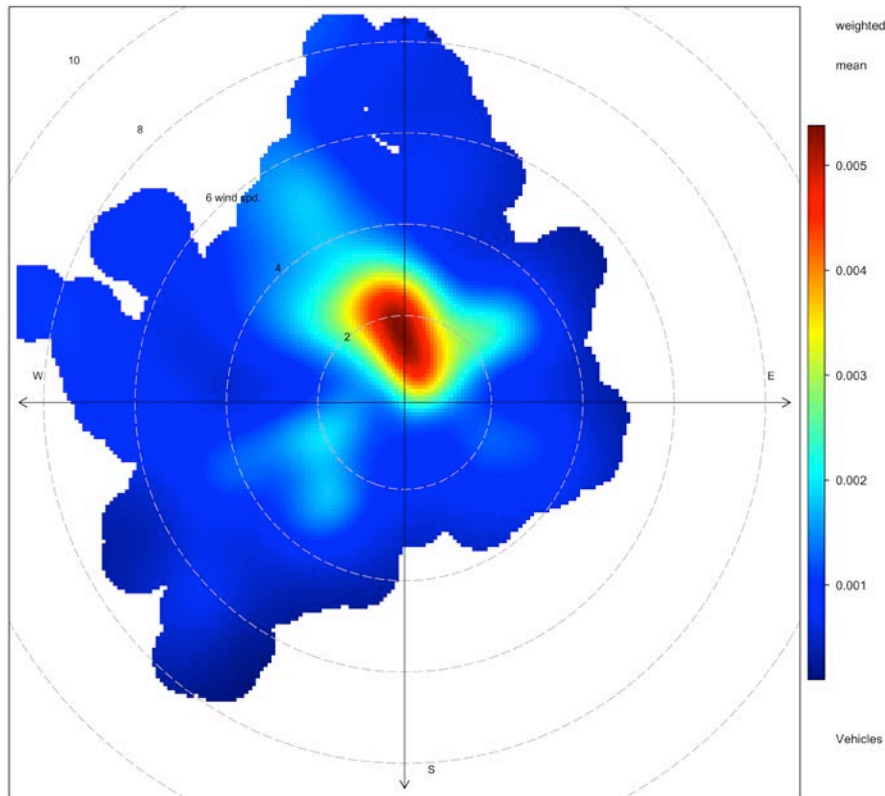


Figure 4.16 Polar plot of motor vehicle contributions. The radial dimensions indicate the wind speed in 2 m s^{-1} increments and the color contours indicate the average contribution to each wind direction/speed bin.

4.5.3 Crustal matter

Crustal matter contributions produced a similar bivariate polar plot to that of motor vehicles (Figure 4.17). Peak contributions tended to occur under moderate wind speeds from the north and were likely related to re-entrained road dust. Since northerly winds prevail at the monitoring site, it is also not unexpected that crustal matter contributions peaked under northerly winds.

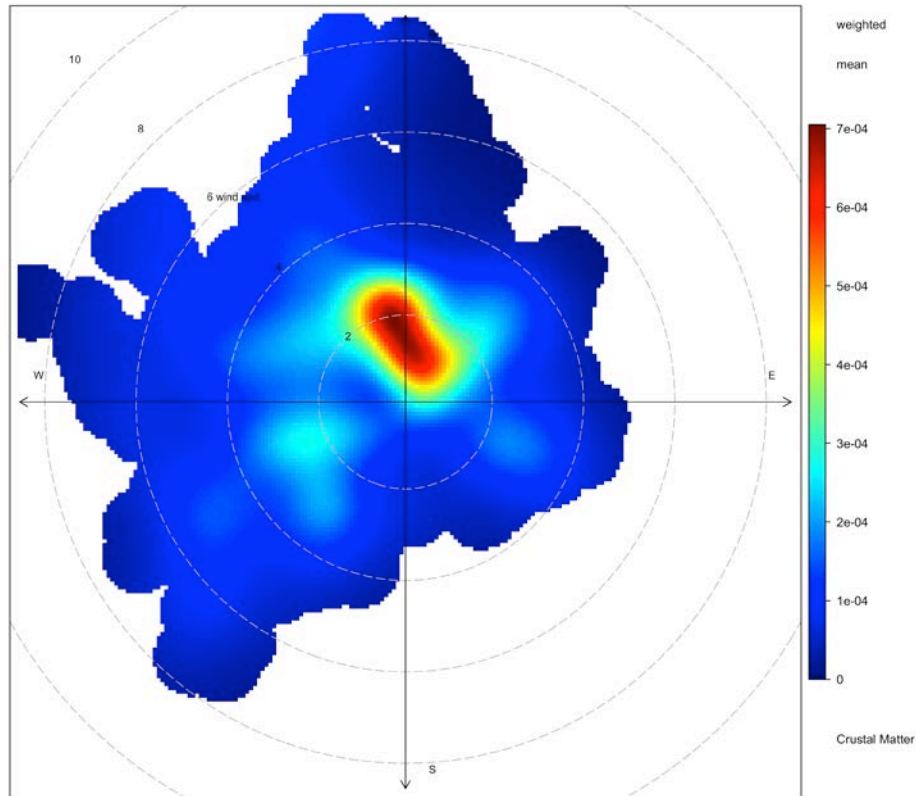


Figure 4.17 Polar plot of crustal matter contributions. The radial dimensions indicate the wind speed in 2 m s^{-1} increments and the color contours indicate the average contribution to each wind direction/speed bin.

4.5.4 Coarse and fine marine aerosol

Figure 4.18 and Figure 4.19 present bivariate polar plots of coarse and fine marine aerosol contributions, respectively. Both source contributions peaked under moderate-to-high southwesterly winds. As such, it is likely that marine aerosol in Invercargill originated from the Foveaux Strait and Southern Ocean.

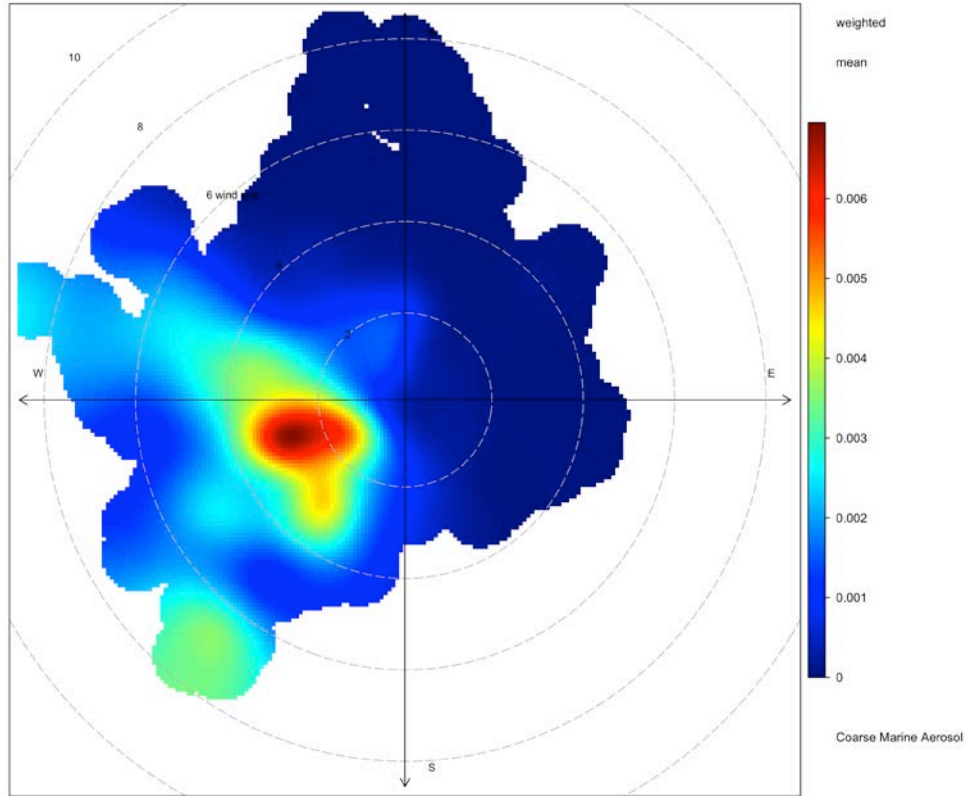


Figure 4.18 Polar plot of coarse marine aerosol contributions. The radial dimensions indicate the wind speed in 2 m s^{-1} increments and the color contours indicate the average contribution to each wind direction/speed bin.

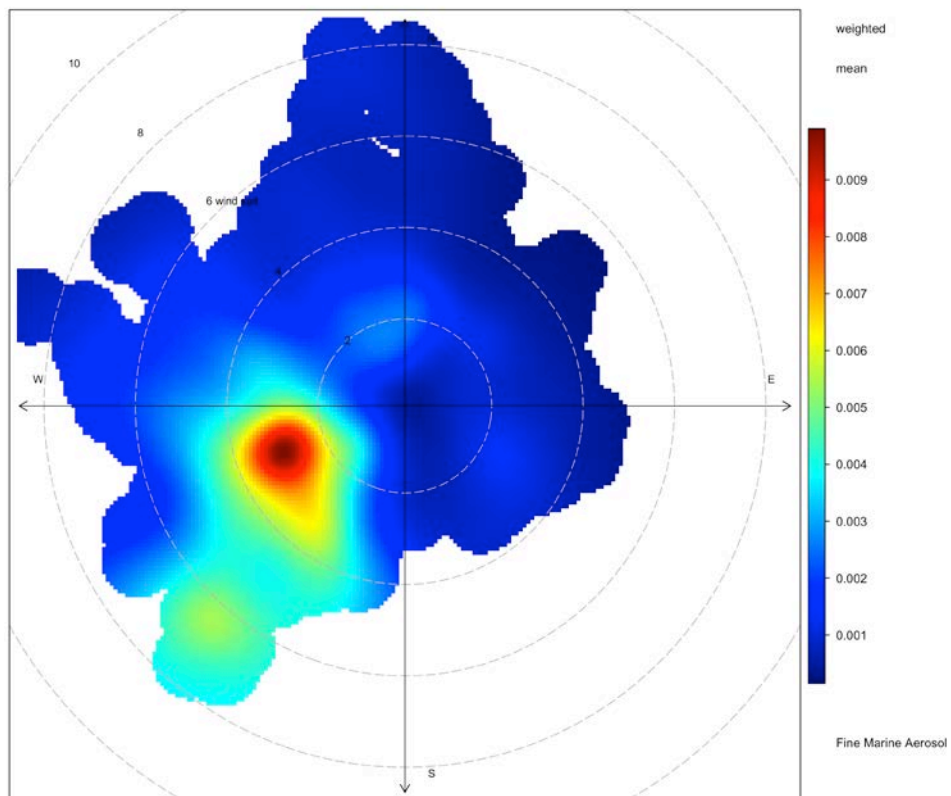


Figure 4.19 Polar plot of fine marine aerosol contributions. The radial dimensions indicate the wind speed in 2 m s^{-1} increments and the color contours indicate the average contribution to each wind direction/speed bin.

This page is intentionally left blank.

5.0 DISCUSSION OF THE FERNWORTH PRIMARY SCHOOL RECEPTOR MODELING RESULTS

Monitoring of hourly, size-resolved PM₁₀ at Fernworth Primary School revealed that the NES for PM₁₀ was exceeded a number of times between 5 June and 22 August 2014. Critically, the diurnal PM₁₀ concentration profile (Figure 3.6) revealed that concentration peaks during the evening and mid-morning were the most responsible for elevated PM₁₀ concentrations. This type of diurnal pattern for PM₁₀ is common throughout New Zealand (Trompetter et al., 2010).

Five source contributors were identified from receptor modeling analysis using PMF. These source contributors showed distinct diurnal cycles and anthropogenic activities were found to dominate PM₁₀ concentrations at Fernworth Primary School. On average, biomass combustion and motor vehicle contributions contributed to 78% of PM₁₀ during this study.

For air quality management purposes, contributions from the various sources to peak PM₁₀ events are of most interest. Therefore, the mass contributions of sources to all PM₁₀ concentrations over 33 µg m⁻³ (the Ministry for the Environment 'Alert' level as discussed in Section 2.1) were evaluated for these days. On these 'alert' days, biomass combustion contributed to 88% of PM₁₀ on average, and up to 93%. Motor vehicles contributed 8% on average, and up to 20%. Combined, these two sources accounted for 96% of PM₁₀ on days when the average PM₁₀ concentration was greater than 33 µg m⁻³.

5.1 SOURCES OF PM₁₀ AT FERNWORTH PRIMARY SCHOOL

5.1.1 Biomass combustion

The biomass combustion source had a diurnal profile similar to that of PM₁₀ because, on average, it accounted for 68% of PM₁₀. The biomass combustion source is related to emissions from solid fuel fires used for domestic heating. It is also likely that the biomass combustion profile contains some contribution from coal combustion. Because these sources are likely to be covariant, more sampling would be required to differentiate these two sources. The possible contribution from coal combustion is indicated from the relatively high sulphur concentration (4% of average sulphur concentration) in the profile. Associated with the biomass combustion profile (Figure 4.1) were arsenic and lead. The presence of arsenic in the biomass combustion profile suggests that CCA-treated timber is being used as part of the domestic fuel stream. This problem is widespread around New Zealand and appears to be opportunistic, that is, CCA-treated timber is used as and when it is available (Ancelet et al., 2014b; 2014a; 2012; Davy et al., 2012). The New Zealand Ambient Air Quality Guidelines (NZAAQG) contain inhalation based health risk guidelines for arsenic species (MfE, 2002). The guideline value for inorganic arsenic is 0.0055 µg m⁻³ (annual average) and for arsine (AsH₃) the guideline value is 0.055 µg m⁻³ (annual average). We assume that arsenic measured in this study is inorganic because arsine decomposes at temperatures above 230 °C. While it is impossible to calculate an annual average concentration of arsenic based on three months of sampling, it is evident that elevated arsenic concentrations occurred. The presence of lead in the profile suggests that residents are also burning lead painted timber in their domestic woodburners. We have recently begun to identify this phenomenon throughout New Zealand as well.

5.1.2 Motor vehicles

Emissions from motor vehicles were found to be a minor contributor to PM₁₀ concentrations (10%). Motor vehicle contributions did not show a weekday/weekend variation, suggesting that the monitoring site is not strongly influenced by commuter traffic. A bivariate polar plot of the motor vehicle contributions revealed that the largest contributions occurred under moderate wind speeds from the north-Northwest and is probably dominated by emissions from traffic in the Invercargill CBD.

5.1.3 Crustal matter

The crustal matter source originates from airborne crustal matter particles, with coarse particles dominating the size range. Soil particles can be generated by wind action or disturbance of surface dusts by motor vehicles, road works or construction activities. At Fernworth Primary School, it is likely that re-entrained road dust and other anthropogenic activities contributed to elevated crustal matter concentrations because weekday contributions tended to be higher than weekend contributions.

5.1.4 Marine aerosol

Two distinct marine aerosol sources were identified, coarse and fine. Together these sources accounted for 21% of PM₁₀ measured at the site. These sources should be considered different because although they were transported to the monitoring site under similar wind speeds and directions, they show different time-series and are likely transported to the monitoring site over different distances. Fine particles tend to be transported much farther than coarse particles, so it is likely that the fine marine aerosol source has aged relative to the coarse marine aerosol source. The average contribution of marine aerosol (2.6 µg m⁻³) was lower than for other areas of New Zealand, including Wainuiomata (5.9 µg m⁻³) and Seaview (6.3 µg m⁻³) in Wellington (Davy et al. 2009a; Davy et al. 2008) and at six Auckland sites (6–7 µg m⁻³) (Davy et al. 2009b). Marine aerosol contributions in a number of locations throughout New Zealand are presented in Figure 5.1. This is likely because this study was only performed during winter, when marine aerosol contributions tend to be lower.

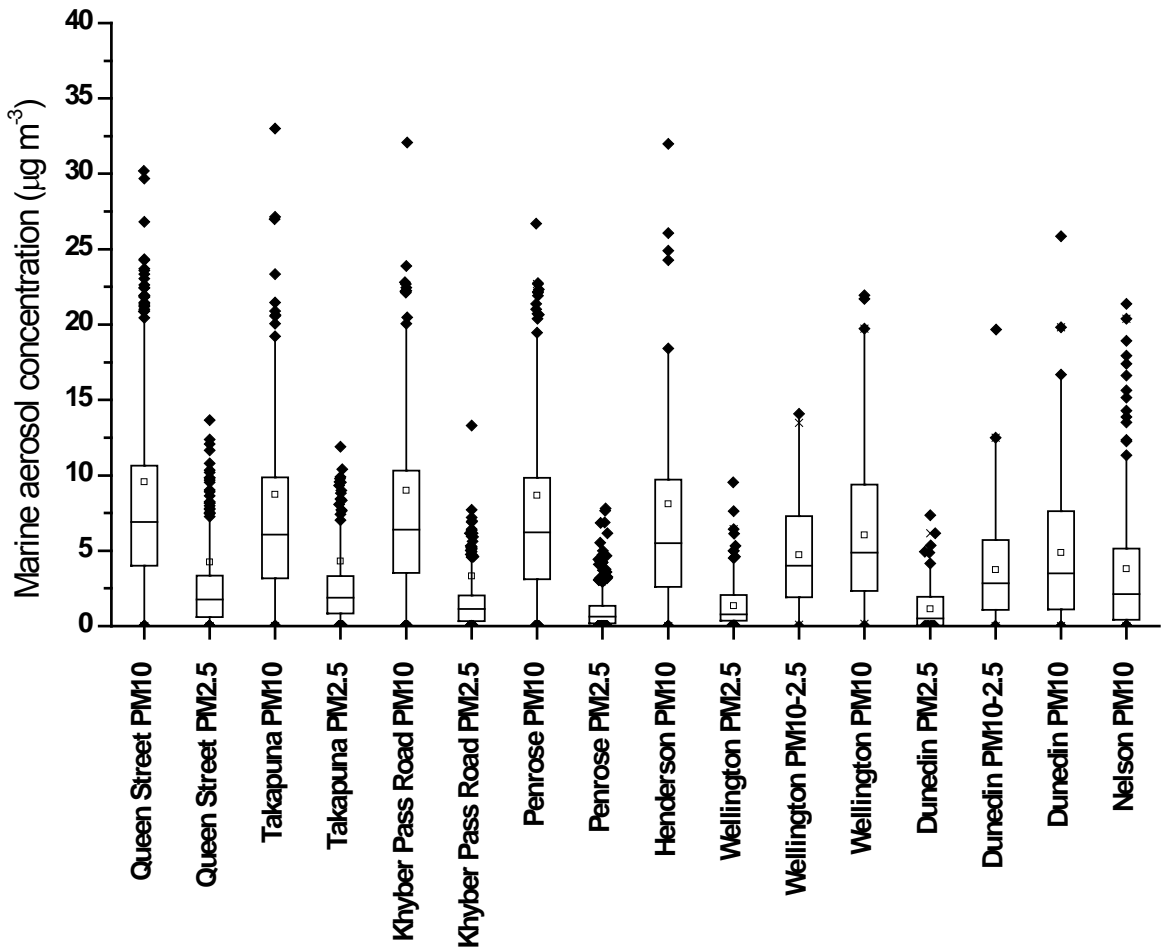


Figure 5.1 Marine aerosol concentrations in a number of New Zealand locations.

This page is intentionally left blank.

This page is intentionally left blank.

6.0 RECOMMENDATIONS

The results of this study provide valuable information about the sources of PM₁₀ at Fernworth Primary School in Invercargill. Based on these results, it is possible for Environment Southland to evaluate options for improving local air quality by targeting a reduction in biomass combustion for home heating. A longer-term PM monitoring campaign could provide useful information about source activity outside of winter. It is possible that with a longer-term study, new sources may be identified that could lead to a greater understanding of the sources and factors that contribute to PM pollution in Invercargill.

The presence of arsenic and lead associated with domestic home heating is a cause for concern. These elements are well-known to be toxic and in addition to their presence in air, it is likely that ashes from fires contain even higher concentrations of these elements. Reducing these emissions, and those of particles in general, is critical for ensuring positive health outcomes for Invercargill residents.

7.0 REFERENCES

- Ancelet, T., Davy, P.K., Mitchell, T., Trompetter, W.J., Markwitz, A., Weatherburn, D.C., 2012. Identification of Particulate Matter Sources on an Hourly Time-Scale in a Wood Burning Community. *Environ. Sci. Technol.* 46, 4767–4774. doi:10.1021/es203937y
- Ancelet, T., Davy, P.K., Trompetter, W.J., Markwitz, A., Weatherburn, D.C., 2014a. Particulate matter sources on an hourly timescale in a rural community during the winter. *Journal of the Air & Waste Management Association* 64, 501–508. doi:10.1080/10962247.2013.813414
- Ancelet, T., Davy, P.K., Trompetter, W.J., Markwitz, A., Weatherburn, D.C., 2014b. Sources and transport of particulate matter on an hourly time-scale during the winter in a New Zealand urban valley. *Urban Climate*. doi:10.1016/j.uclim.2014.06.003
- Annegarn, H. J., Cahill, T. A., Sellschop, J. F. P., Zucchiatti, A., 1988 Time sequence particulate sampling and nuclear analysis. *Physics Scripta* 37, 282–290.
- Annegarn, H.J., Flanz, M., Kenntner, T., Kneen, M.A., Helas, G., Piketh, S.J., 1996. Airborne streaker sampling for PIXE analysis. *Nuclear Inst. and Methods in Physics Research, B* 109, 548–550.
- Begum, B.A., Hopke, P.K., Zhao, W.X., 2005. Source identification of fine particles in Washington, DC, by expanded factor analysis modeling. *Environ. Sci. Technol.* 39, 1129–1137.
- Brown, S.G., Hafner, H.R., (2005). *Multivariate Receptor Modelling Workbook*. USEPA, Research Triangle Park, NC.
- Cahill, T.A., Eldred, R.A., Motallebi, N., Malm, W.C., 1989. Indirect measurement of hydrocarbon aerosols across the United States by nonsulfate hydrogen-remaining gravimetric mass correlations. *Aerosol Sci. Technol.* 10, 421–429.
- Carslaw, D.C., Ropkins, K., 2012. openair - An R package for air quality data analysis. *Environmental Modelling and Software* 27–28, 52–61. doi:10.1016/j.envsoft.2011.09.008
- Chueinta, W., Hopke, P.K., Paatero, P., 2000. Investigation of sources of atmospheric aerosol at urban and suburban residential areas in Thailand by positive matrix factorization. *Atmos. Environ.* 34, 3319–3329.
- Cohen, D., Bailey, G., Kondepudi, R., 1996. Elemental analysis by PIXE and other IBA techniques and their application to source fingerprinting of atmospheric fine particle pollution. *Nucl. Inst. Meth. Phys. Res. B* 109/110, 218–226.
- Cohen, D., 1998. Characterisation of atmospheric fine particles using IBA techniques. *Nucl. Inst. Meth. Phys. Res. B* 136–138, 14–22.
- Cohen, D.D., 1999. Accelerator based ion beam techniques for trace element aerosol analysis. *Advances in Environmental, Industrial and Process Control Technologies* 1, 139–196.
- Cohen, D., Taha, G., Stelcer, E., Garton, D., Box, G., (2000). The measurement and sources of fine particle elemental carbon at several key sites in NSW over the past eight years. *15th Clean Air Conference*, Clean air Society of Australia and New Zealand, Sydney.
- Davy, P.K., Ancelet, T., Trompetter, W.J., Markwitz, A., Weatherburn, D.C., 2012. Composition and source contributions of air particulate matter pollution in a New Zealand suburban town. *Atmospheric Pollution ...* 3, 143–147. doi:10.5094/APR.2012.014
- Davy, P., K., Trompetter, W., Markwitz, A., (2009a). Source apportionment of airborne particles at Wainuiomata, Lower Hutt. GNS Science Client Report 2009/188, Wellington.
- Davy, P., K., Trompetter, W., Markwitz, A., (2009b). Source apportionment of airborne particles in the Auckland region: 2008 Update. GNS Science Client Report 2009/165, Wellington.

- Davy, P., K., Trompetter, W.J., Markwitz, A., (2008). Source apportionment of airborne particles at Seaview, Lower Hutt. GNS Science Client Report 2008/160, Wellington.
- Eberly, S., (2005). EPA PMF 1.1 User's Guide. USEPA.
- Fine, P.M., Cass, G.R., Simoneit, B.R., 2001. Chemical characterization of fine particle emissions from fireplace combustion of woods grown in the northeastern United States. *Environ. Sci. Technol.* 35, 2665-2675.
- Hopke, P.K., Xie, Y.L., Paatero, P., 1999. Mixed multiway analysis of airborne particle composition data. *J. Chemomet.* 13, 343-352.
- Horvath, H., 1993. Atmospheric Light Absorption - A Review. *Atmos. Environ*, 27A, 293-317.
- Horvath, H., 1997. Experimental calibration for aerosol light absorption measurements using the integrating plate method - Summary of the data. *Aerosol Science* 28, 2885-2887.
- Jacobson, M.C., Hansson, H.C., Noone, K.J., Charlson, R.J., 2000. Organic atmospheric aerosols: review and state of the science. *Reviews of Geophysics* 38, 267-294.
- Jeong, C.-H., Hopke, P.K., Kim, E., Lee, D.-W., 2004. The comparison between thermal-optical transmittance elemental carbon and Aethalometer black carbon measured at multiple monitoring sites. *Atmos. Environ.* 38, 5193.
- Kim, E., Hopke, P.K., Edgerton, E.S., 2003. Source identification of Atlanta aerosol by positive matrix factorization. *J. Air Waste Manage. Assoc.* 53, 731-739.
- Kim, E., Hopke, P.K., Larson, T.V., Maykut, N.N., Lewtas, J., 2004. Factor analysis of Seattle fine particles. *Aerosol Sci. Technol.* 38, 724-738.
- Lee, E., Chan, C.K., Paatero, P., 1999. Application of positive matrix factorization in source apportionment of particulate pollutants in Hong Kong. *Atmos. Environ*, 33, 3201-3212.
- Lee, J.H., Yoshida, Y., Turpin, B.J., Hopke, P.K., Poirot, R.L., Lioy, P.J., Oxley, J.C., 2002. Identification of sources contributing to Mid-Atlantic regional aerosol. *J. Air Waste Manag. Assoc.* 52, 1186-1205.
- Maenhaut, W., Malmqvist, K., G., Particle Induced X-ray Emission Analysis. In: R.V. Grieken, Editor, *Handbook of x-ray spectrometry*, Marcel Dekker Inc., Antwerp (2001).
- Malm, W.C., Sisler, J.F., Huffman, D., Eldred, R.A., Cahill, T.A., 1994. Spatial and seasonal trends in particle concentration and optical extinction in the United States. *J. Geophys. Res. Atmos.* 99, 1347-1370.
- Maxwell, J.A., Cambell, J.L., Teesdale, W.J., 1989. The Guelph PIXE software package. *Nucl. Instr. And Meth. B* 43, 218.
- Maxwell, J.A., Teesdale, W.J., Cambell, J.L., 1995. The Guelph PIXE software package II. *Nucl. Instr. And Meth. B* 95, 407.
- Ministry for the Environment, (2002). New Zealand Ambient Air Quality Guidelines. New Zealand Government, Wellington
- Paatero, P., 1997. Least squares formulation of robust non-negative factor analysis. *Chemom. Intell. Lab. Syst.* 18, 183-194.
- Paatero, P., (2000). PMF User's Guide. University of Helsinki, Helsinki.
- Paatero, P., Hopke, P.K., 2002. Utilizing wind direction and wind speed as independent variables in multilinear receptor modeling studies. *Chemometrics and Intelligent Laboratory Systems* 60, 25-41.

- Paatero, P., Hopke, P.K., 2003. Discarding or downweighting high-noise variables in factor analytic models. *Analytica Chimica Acta* 490, 277-289.
- Paatero, P., Hopke, P.K., Begum, B.A., Biswas, S.K., 2005. A graphical diagnostic method for assessing the rotation in factor analytical models of atmospheric pollution. *Atmospheric Environment* 39, 193-201.
- R Development Core Team, (2011). R: A language and environment for statistical computing. R Foundation for Statistical Computing, Vienna, Austria.
- Ramadan, Z., Eickhout, B., Song, X.-H., Buydens, L.M.C., Hopke, P.K., 2003. Comparison of Positive Matrix Factorization and Multilinear Engine for the source apportionment of particulate pollutants. *Chemomet. Intellig. Lab. Syst.* 66, 15-28.
- Salma, I., Chi, X., Maenhaut, W., 2004. Elemental and organic carbon in urban canyon and background environments in Budapest, Hungary. *Atmos. Environ.* 38, 27-36.
- Scott, A.J., (2006). Source Apportionment and Chemical Characterisation of Airborne Fine Particulate Matter in Christchurch, New Zealand. University of Canterbury, Christchurch.
- Song, X.H., Polissar, A.V., Hopke, P.K., 2001. Sources of fine particle composition in the northeastern US. *Atmospheric Environment* 35, 5277-5286.
- Trompetter, W.J., (2004). Ion Beam Analysis results of air particulate filters from the Wellington Regional Council. Geological and Nuclear Sciences Limited, Wellington.
- Trompetter, W.J., Davy, P.K., (2005). Air Particulate Research Capability at the New Zealand Ion Beam Analysis facility using PIXE and IBA techniques. *BioPIXE 5*, Wellington, New Zealand.
- Trompetter, W.J., Davy, P.K., Markwitz, A., 2010. Influence of environmental conditions on carbonaceous particle concentrations within New Zealand. *Journal of Aerosol Science* 41, 134–142. doi:10.1016/j.jaerosci.2009.11.003
- Watson, J.G., Zhu, T., Chow, J.C., Engelbrecht, J., Fujita, E.M., Wilson, W.E., 2002. Receptor modeling application framework for particle source apportionment. *Chemosphere* 49, 1093-1136.
- WHO, (2006). Air quality guidelines. Global update 2005.

APPENDICES

This page is intentionally left blank.

A1.0 APPENDIX 1: ANALYSIS TECHNIQUES

A1.1 ELEMENTAL ANALYSIS OF AIRBORNE PARTICLES

A1.1.1 Ion beam analysis

Ion beam analysis (IBA) was used to measure the elemental concentrations of particulate matter on the size-resolved filter samples from the Pomona Street monitoring site shown in Figure 2.1. IBA is based on the measurement of characteristic X-rays and γ -rays of an element produced by ion-atom interactions using high-energy protons in the 2–5 million electron volt (MeV) range. IBA is a mature and well developed science, with many research groups around the world using IBA in a variety of routine analytical applications, including the analysis of atmospheric aerosols (Maenhaut and Malmqvist, 2001; Trompetter et al., 2005). IBA techniques do not require sample preparation and are fast, non-destructive and sensitive (Cohen, 1999; Maenhaut and Malmqvist, 2001; Trompetter et al., 2005).

IBA measurements for this study were carried out at the New Zealand IBA facility operated by GNS Science. Figure A1.1 shows the PM analysis chamber with its associated X-ray, γ -ray and particle detectors for Proton-Induced X-ray Emission (PIXE), Proton-Induced Gamma-ray Emission (PIGE), Proton Elastic Scattering Analysis (PESA) and Rutherford BackScattering (RBS) measurements.

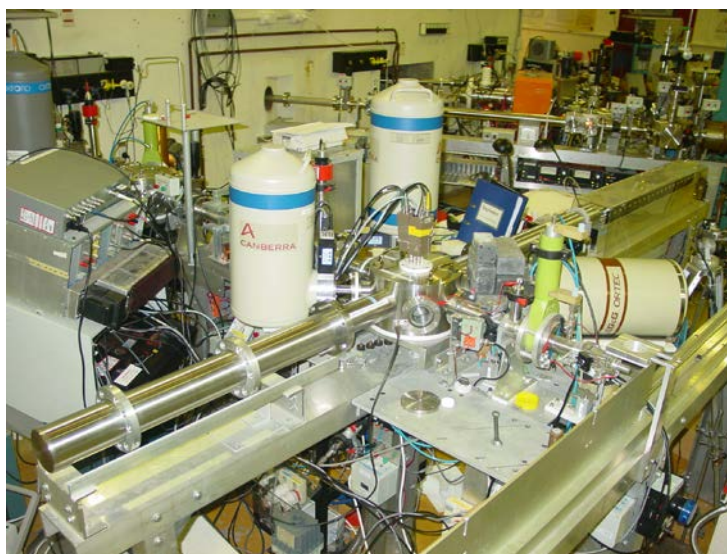


Figure A1.1 Particulate matter analysis chamber with its associated detectors.

The following sections provide a generalised overview of the IBA techniques used for elemental analysis and the analytical setup at GNS Science (Cohen, 1998; Cohen et al., 1996; Trompetter, 2004; Trompetter and Davy, 2005). Figure A2.2 presents a schematic diagram of the typical experimental setup for IBA of air particulate filters at GNS Science.

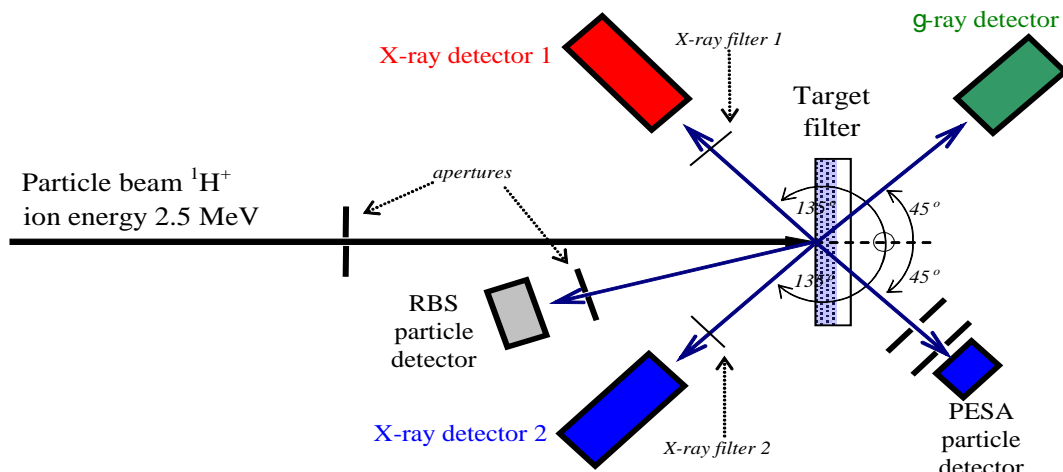


Figure A1.2 Schematic of the typical IBA experimental setup at GNS Science.

A1.1.1.1 Particle-induced X-ray emission

Particle induced X-ray emission (PIXE), is used to determine elemental concentrations heavier than neon by exposing the filter samples to a proton beam accelerated to 2.5 million volts (MeV) by the GNS 3 MeV van-de-Graaff accelerator. When high energy protons interact with atoms in the sample, characteristic X-rays (from each element) are emitted by ion-electron processes. These X-rays are recorded in an energy spectrum. While all elements heavier than boron emit K X-rays, their production become too few to satisfactorily measure elements heavier than strontium. Elements heavier than strontium are detected via their lower energy L X-rays. The X-rays are detected using a Si(Li) detector and the pulses from the detector are amplified and recorded in a pulse height analyser. In practice, sensitivities are further improved for the lighter elements by using two X-ray detectors, one for light element X-rays and the other for heavier element X-rays, each with different filtering and collimation. Figure A1.3 shows an example of a PIXE spectrum for airborne particles collected on a filter and analysed at the GNS IBA facility.

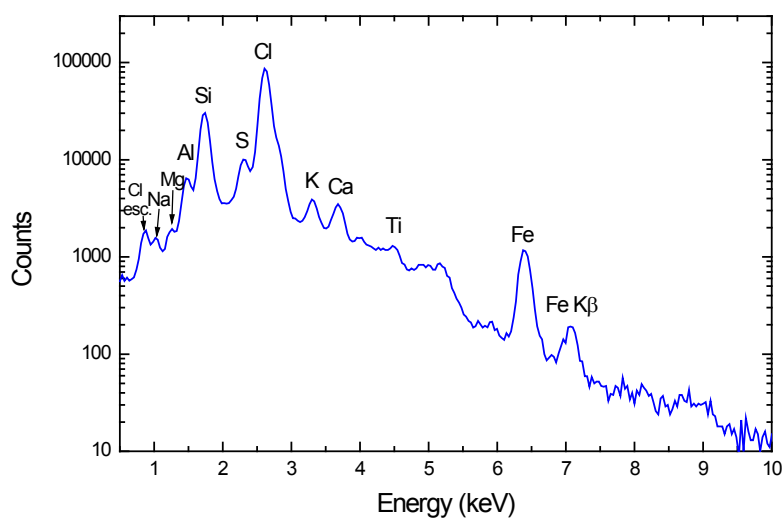


Figure A1.3 Typical PIXE spectrum for an aerosol sample analysed by PIXE.

As the PIXE spectrum consists of many peaks from different elements (and a Bremsstrahlung background), some of them overlapping, the spectrum is analysed with quantitative X-ray analysis software. In the case of this study, Gupix Software was used to perform the deconvolution with high accuracy (Maxwell et al., 1989; Maxwell et al., 1995). The number of pulses (counts) in each peak for a given element is used by the Gupix software to calculate the concentration of that element. The background and neighbouring elements determine the statistical error and the limit of detection. Note, that Gupix provides a specific statistical error and limit of detection (LOD) for each element in any filter, which is essential for source apportionment studies.

Typically 20–25 elements from Mg–Pb are routinely determined above their respective LODs. Sodium (and fluorine) was determined using both PIXE and PIGE (see next section). Specific experimental details, where appropriate, are given in the results and analysis section.

A1.1.1.2 Particle-induced gamma-ray emission

Particle Induced Gamma-Ray Emission (PIGE) refers to γ -rays produced when an incident beam of protons interacts with the nuclei of an element in the sample (filter). During the de-excitation process, nuclei emit γ -ray photons of characteristic energies specific to each element. Typical elements measured with γ -ray are:

<i>Element</i>	<i>nuclear reaction</i>	<i>gamma ray energy (keV)</i>
Sodium	$^{23}\text{Na}(p,\alpha\gamma)^{20}\text{Ne}$	440, 1634
Fluorine	$^{19}\text{F}(p,\alpha\gamma)^{16}\text{O}$	197, 6129

Gamma rays are higher in energy than X-rays and are detected with a germanium detector. Measurements of a light element such as sodium can be measured more accurately using PIGE because the γ -rays are not attenuated to the same extent in the filter matrix or the detector material, a problem in the measurement of low energy X-rays of sodium. Figure A1.4 shows a typical PIGE spectrum.

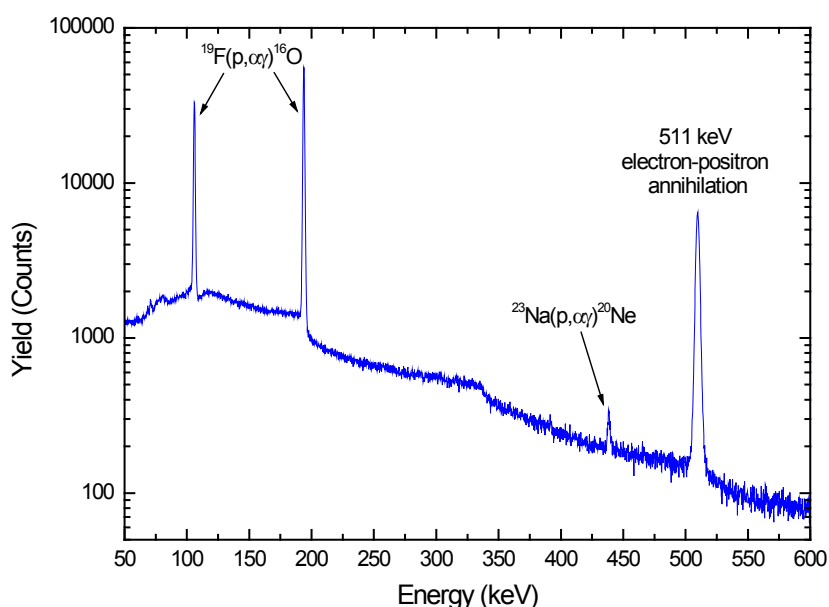


Figure A1.4 Typical PIGE spectrum for an aerosol sample.

A1.1.1.3 Particle elastic scattering analysis

Particle Elastic Scattering Analysis (PESA) allows hydrogen to be measured quantitatively in air particulate matter collected on a filter providing the filter material contains no or little hydrogen atoms, e.g., Teflon filters. Note that Teflon contains fluorine that introduces a significant background in the X-ray spectra which increases the limits of detection (LODs) of PIXE. Hydrogen can be detected by measuring the elastically scattered protons in a forward direction for a proton beam passing through the air particulate matter filter. At a forward scattering angle of 45°, the protons are elastically scattered from hydrogen with 50% of the initial proton energy (i.e., for an incident beam of 2.50 MeV the energy of protons scattered off hydrogen is 1.25 MeV) which is much less energy than the energy of the protons scattered from the other heavier elements in the filter. Thus, in the PESA spectrum of a sample filter, a peak corresponding to protons elastically scattered from hydrogen occurs separated from the protons elastically scattered from the other atoms in the air particulate matter filter. The air particulate matter filter is thin enough for this measurement when the hydrogen PESA peak is separated from the noise at the low end of the spectrum and from protons elastically scattered from heavier atoms at the high energy end of the spectrum. For Teflon filters analysed with a 2.5 MeV proton beam, proton scattering energies for PESA are shown in Table A1.1 and Figure A1.5 presents a typical PESA spectrum.

Table A1.1 Proton scattering energies of various elements for a 2.5MeV proton beam.

Element	Energy detected at 45° forward (MeV)
H	1.250
C	2.380
O	2.410
F	2.424
Fe	2.474

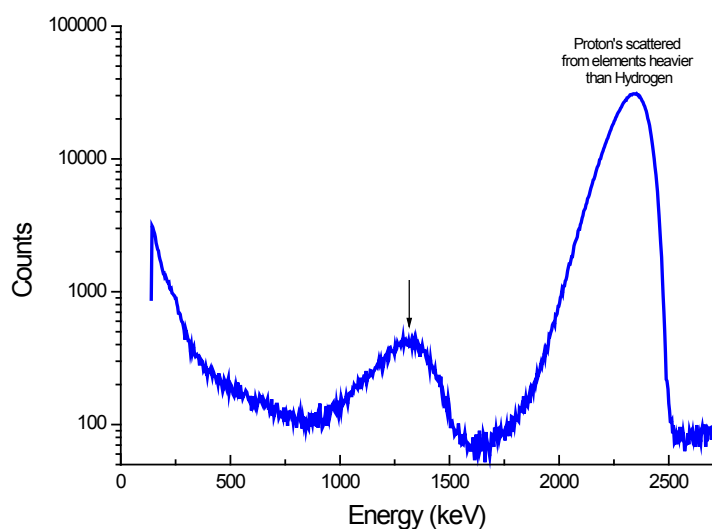


Figure A1.5 PESA spectrum for an aerosol sample showing the hydrogen peak at 1.250 MeV.

Because PESA, and IBA measurements in general, are conducted in high vacuum (residual gas pressure better than 10^{-6} mbar), free water vapour and VOCs are volatilised before analysis and only bound hydrogen is detected (e.g., SVOCs and ammonium ions) (Cohen, 1999).

A1.1.1.4 IBA data reporting

Most filters used to collect particulate matter samples for IBA analysis are sufficiently thin that the ion beam penetrates the entire depth producing a quantitative analysis of elements present. Because of the thin nature of the air particulate matter filters, the concentrations reported from the IBA analyses are therefore in aerial density units (ng cm^{-2}) and the total concentration of each element on the filters is calculated by multiplying with the exposed area of the filter. Typically the exposed area is 0.16 cm^2 for filters collected with the Streaker sampler used in this study. For example, to convert from $\text{Cl} (\text{ng cm}^{-2})$ into $\text{Cl} (\text{ng m}^{-3})$ for filter samples, the equation is:

$$\text{Cl} (\text{ng m}^{-3}) = 0.16 (\text{cm}^2) \times \text{Cl} (\text{ng cm}^{-2}) / \text{Vol}(\text{m}^3) \quad \text{Equation A1.1}$$

A1.1.1.5 Limits of detection for elements determined by IBA

The exact limits of detection for reporting the concentration of each element depends on a number of factors such as:

- the method of detection;
- filter composition;
- sample composition;
- the detector resolution;
- spectral interference from other elements.

To determine the concentration of each element the background is subtracted and peak areas fitted and calculated. The background occurs through energy loss, scattering and interactions of the ion beam as it passes through the filter material or from γ -rays produced in the target and scattered in the detector system (Cohen, 1999). The peaks of elements in spectra that have interferences or backgrounds from other elements present in the air particulate matter, or filter matrix itself, will have higher limits of detection. Choice of filter material is an important consideration with respect to elements of interest as is avoiding sources of contamination. The GNS IBA laboratory routinely runs filter blanks to correct for filter derived analytical artefacts as part of their QA/QC procedures. Figure A1.6 shows the LODs typically achieved by PIXE for each element at the GNS IBA facility. All IBA elemental concentrations determined in this work were accompanied by their respective LODs. The use of elemental LODs is important in receptor modeling applications and is discussed further in Section A1.4.2.

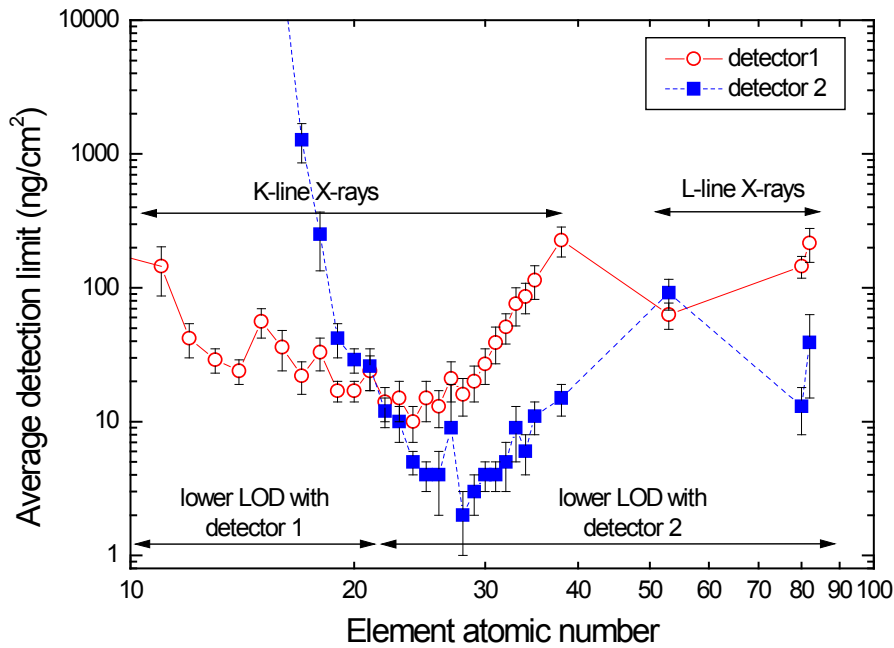


Figure A1.6 Elemental limits of detection for PIXE routinely achieved as the GNS IBA facility for air filters.

A1.2 BLACK CARBON MEASUREMENTS

Black carbon (BC) has been studied extensively, but it is still not clear to what degree it is elemental carbon (EC (or graphitic) C(0)) or high molecular weight refractory weight organic species or a combination of both (Jacobson et al., 2000). Current literature suggests that BC is likely a combination of both, and that for combustion sources such as petrol and diesel fuelled vehicles and biomass combustion (wood burning, coal burning), EC and organic carbon compounds (OC) are the principle aerosol components emitted (Fine et al., 2001; Jacobson et al., 2000; Salma et al., 2004; Watson et al., 2002).

Determination of carbon (soot) on filters was performed by light reflection to provide the BC concentration. The absorption and reflection of visible light on particles in the atmosphere or collected on filters is dependent on the particle concentration, density, refractive index and size. For atmospheric particles, BC is the most highly absorbing component in the visible light spectrum with very much smaller components coming from soils, sulphates and nitrate (Horvath, 1993, 1997). Hence, to the first order it can be assumed that all the absorption on atmospheric filters is due to BC. The main sources of atmospheric BC are anthropogenic combustion sources and include biomass burning, motor vehicles and industrial emissions (Cohen et al., 2000). Cohen and co-workers found that BC is typically 10–40% of the fine mass (PM_{2.5}) fraction in many urban areas of Australia.

When measuring BC by light reflection/transmission, light from a light source is transmitted through a filter onto a photocell. The amount of light absorption is proportional to the amount of black carbon present and provides a value that is a measure of the black carbon on the filter. Conversion of the absorbance value to an atmospheric concentration value of BC requires the use of an empirically derived equation (Cohen et al., 2000):

$$BC (\mu\text{g cm}^{-2}) = (100/2(F\varepsilon)) \ln[R_0/R] \quad \text{Equation A1.2}$$

where:

ε is the mass absorbent coefficient for BC ($\text{m}^2 \text{g}^{-1}$) at a given wavelength;

F is a correction factor to account for other absorbing factors such as sulphates, nitrates, shadowing and filter loading. These effects are generally assumed to be negligible and F is set at 1.00;

R_0, R are the pre- and post-reflection intensity measurements, respectively.

Black carbon was measured at GNS Science using the M43D Digital Smoke Stain Reflectometer. The following equation (from Willy Maenhaut, Institute for Nuclear Sciences, University of Gent Proeftuinstraat 86, B-9000 GENT, Belgium) was used for obtaining BC from reflectance measurements on Nucleopore polycarbonate filters or Pall Life Sciences Teflon filters:

$$BC (\mu\text{g cm}^{-2}) = [1000 \times \text{LOG}(R_{\text{blank}}/R_{\text{sample}}) + 2.39] / 45.8 \quad \text{Equation A1.3}$$

where:

R_{blank} : the average reflectance for a series of blank filters; R_{blank} is close (but not identical) to 100. GNS always use the same blank filter for adjusting to 100.

R_{sample} : the reflectance for a filter sample (normally lower than 100).

With: 2.39 and 45.8 constants derived using a series of 100 Nucleopore polycarbonate filter samples which served as secondary standards; the BC loading (in $\mu\text{g cm}^{-2}$) for these samples had been determined by Prof. Dr. M.O. Andreae (Max Planck Institute of Chemistry, Mainz, Germany) relative to standards that were prepared by collecting burning acetylene soot on filters and determining the mass concentration gravimetrically (Trompeter, 2004).

A1.3 POSITIVE MATRIX FACTORISATION

Positive matrix factorisation (PMF) is a linear least-squares approach to factor analysis and was designed to overcome the receptor modeling problems associated with techniques like principal components analysis (PCA) (Paatero et al., 2005). With PMF, sources are constrained to have non-negative species concentrations, no sample can have a negative source contribution and error estimates for each observed data point are used as point-by-point weights. This feature is a distinct advantage, in that it can accommodate missing and below detection limit data that is a common feature of environmental monitoring results (Song et al., 2001). In fact, the signal to noise ratio for an individual elemental measurement can have a significant influence on a receptor model and modeling results. For the weakest (closest to detection limit) species, the variance may be entirely from noise (Paatero and Hopke, 2002). Paatero and Hopke strongly suggest down-weighting or discarding noisy variables that are always below their detection limit or species that have a lot of error in their measurements relative to the magnitude of their concentrations (Paatero and Hopke, 2003). The distinct advantage of PMF is that mass concentrations can be included in the model and the results are directly interpretable as mass contributions from each factor (source).

A1.3.1 PMF model outline

The mathematical basis for PMF is described in detail by Paatero (Paatero, 1997, 2000). Briefly, PMF uses a weighted least-squares fit with the known error estimates of measured elemental concentrations used to derive the weights. In matrix notation this is indicated as:

$$X = GF + E \quad \text{Equation A1.4}$$

where:

X is the known $n \times m$ matrix of m measured elemental species in n samples;

G is an $n \times p$ matrix of source contributions to the samples;

F is a $p \times m$ matrix of source compositions (source profiles).

E is a residual matrix – the difference between measurement X and model Y .

E can be defined as a function of factors G and F :

$$e_{ij} = x_{ij} - y_{ij} = x_{ij} - \sum_{k=1}^p g_{ik} f_{kj} \quad \text{Equation A1.5}$$

where:

$i = 1, \dots, n$ elements

$j = 1, \dots, m$ samples

$k = 1, \dots, p$ sources

PMF constrains all elements of G and F to be non-negative, meaning that elements cannot have negative concentrations and samples cannot have negative source contributions as in real space. The task of PMF is to minimise the function Q such that:

$$Q(E) = \sum_{i=1}^n \sum_{j=1}^m (e_{ij} / \sigma_{ij})^2 \quad \text{Equation A1.6}$$

where σ_{ij} is the error estimate for x_{ij} . Another advantage of PMF is the ability to handle extreme values typical of air pollutant concentrations as well as true outliers that would normally skew PCA. In either case, such high values would have significant influence on the solution (commonly referred to as leverage). PMF has been successfully applied to receptor modeling studies in a number of countries around the world (Begum et al., 2005; Chueinta et al., 2000; Hopke et al., 1999; Jeong et al., 2004; Kim et al., 2003; Kim et al., 2004; Lee et al., 1999; Lee et al., 2002; Song et al., 2001) including New Zealand (Ancelet et al., 2012; Davy, 2007; Davy et al., 2009a, b; Davy et al., 2007, 2008; Scott, 2006).

A1.3.2 PMF model used

Two programs have been written to implement different algorithms for solving the least squares PMF problem, these are PMF2 and EPAPMF, which incorporates the Multilinear Engine (ME-2) (Hopke et al., 1999; Ramadan et al., 2003). In effect, the EPAPMF program provides a more flexible framework than PMF2 for controlling the solutions of the factor analysis with the ability of imposing explicit external constraints.

This study used EPAPMF 3.0 (version 3.0.2.2), which incorporates a graphical user interface (GUI) based on the ME-2 program. Both PMF2 and EPAPMF programs can be operated in a robust mode, meaning that “outliers” are not allowed to overly influence the fitting of the contributions and profiles (Eberly, 2005). The user specifies two input files, one file with the concentrations and one with the uncertainties associated with those concentrations. The methodology for developing an uncertainty matrix associated with the elemental concentrations for this work is discussed in Section A1.4.2.

A1.3.3 PMF model inputs

The PMF programs provide the user with a number of choices in model parameters that can influence the final solution. Two parameters, the ‘signal-to-noise ratio’ and the ‘species category’ are of particular importance and are described below.

Signal-to-noise ratio - this is a useful diagnostic statistic estimated from the input data and uncertainty files using the following calculation:

$$(1/2) \sqrt{\frac{\sum_{i=1}^n (x_{ij})^2}{\sum_{i=1}^n (\sigma_{ij})^2}}$$

Equation A1.7

Where x_{ij} and σ_{ij} are the concentration and uncertainty, respectively, of the i^{th} element in the j^{th} sample. Smaller signal-to-noise ratios indicate that the measured elemental concentrations are generally near the detection limit and the user should consider whether to include that species in the receptor model or at least strongly down-weight it (Paatero and Hopke, 2003). The signal-to-noise ratios (S/N ratio) for each element are reported alongside other statistical data in the results section.

Species category - this enables the user to specify whether the elemental species should be considered:

- Strong – whereby the element is generally present in concentrations well above the LOD (high signal to noise ratio) and the uncertainty matrix is a reasonable representation of the errors.
- Weak – where the element may be present in concentrations near the LOD (low signal to noise ratio); there is doubt about some of the measurements and/or the error estimates; or the elemental species is only detected some of the time. If ‘Weak’ is chosen EPA.PMF increases the user-provided uncertainties for that variable by a factor of 3.
- Bad – that variable is excluded from the model run.

For this work, an element with concentrations at least 3 times above the LOD, a high signal to noise ratio (> 2) and present in all samples was considered 'Strong'. Variables were labelled as weak if their concentrations were generally low, had a low signal to noise ratio, were only present in a few samples or there was a lower level of confidence in their measurement. Mass concentration gravimetric measurements and BC were also down weighted as 'Weak' because their concentrations are generally several orders of magnitude above other species, which can have the tendency to 'pull' the model. Paatero and Hopke recommend that such variables be down weighted and that it doesn't particularly affect the model fitting if those variables are from real sources (Paatero and Hopke, 2003). What does affect the model severely is if a dubious variable is over-weighted. Elements that had a low signal to noise ratio (< 0.2), or had mostly missing (zero) values, or were doubtful for any reason, were labelled as 'Bad' and were subsequently not included in the analyses.

If the model is appropriate for the data and if the uncertainties specified are truly reflective of the uncertainties in the data, then Q (according to Eberly) should be approximately equal to the number of data points in the concentration data set (Eberly, 2005):

$$\textit{Theoretical } Q = \# \textit{ samples } \times \# \textit{ species measured} \quad \textbf{Equation A1.8}$$

However, a slightly different approach to calculating the Theoretical Q value was recommended by (Brown and Hafner, 2005), which takes into account the degrees of freedom in the PMF model and the additional constraints in place for each model run. This theoretical Q calculation Q_{th} is given as:

$$Q_{th} = (\# \textit{ samples } \times \# \textit{ good species}) + [(\# \textit{ samples } \times \# \textit{ weak species}) / 3] - (\# \textit{ samples } \times \textit{ factors estimated}) \quad \textbf{Equation A1.9}$$

Both approaches have been taken into account for this study and it is likely that the actual value lies somewhere between the two.

In PMF, it is assumed that only the x_{ij} 's are known and that the goal is to estimate the contributions (g_{jk}) and the factors (or profiles) (f_{kj}). It is assumed that the contributions and mass fractions are all non-negative, hence the "constrained" part of the least-squares. Additionally, EPAPMF allows the user to say how much uncertainty there is in each x_{ij} . Species-days with lots of uncertainty are not allowed to influence the estimation of the contributions and profiles as much as those with small uncertainty, hence the "weighted" part of the least squares and the advantage of this approach over PCA.

Diagnostic outputs from the PMF models were used to guide the appropriateness of the number of factors generated and how well the receptor modelling was accounting for the input data. Where necessary, initial solutions have been 'rotated' to provide a better separation of factors (sources) that were considered physically reasonable (Paatero et al., 2002). Each PMF model run reported in this study is accompanied by the modelling statistics along with comments where appropriate.

A1.4 DATASET QUALITY ASSURANCE

Quality assurance of sample elemental datasets is vital so that any dubious samples, measurements and outliers are removed as these will invariably affect the results of receptor modelling. In general, the larger the dataset used for receptor modelling, the more robust the analysis. The following sections describe the methodology used to check data integrity and provide a quality assurance process that ensured that the data being used in subsequent factor analysis was as robust as possible.

A1.4.1 Mass reconstruction and mass closure

Once the sample analysis for the range of analytes has been carried out, it is important to check that total measured mass does not exceed gravimetric mass (Cohen, 1999). Ideally, when elemental analysis and organic compound analysis has been undertaken on the same sample one can reconstruct the mass using the following general equation for ambient samples as a first approximation (Cahill et al., 1989; Cohen, 1999; Malm et al., 1994):

$$\text{Reconstructed mass} = [\text{Soil}] + [\text{OC}] + [\text{BC}] + [\text{Smoke}] + [\text{Sulphate}] + [\text{Seasalt}]$$

Equation A1.10

where:

$$[\text{Soil}] = 2.20[\text{Al}] + 2.49[\text{Si}] + 1.63[\text{Ca}] + 2.42[\text{Fe}] + 1.94[\text{Ti}]$$

$$[\text{OC}] = \Sigma[\text{Concentrations of organic compounds}]$$

$$[\text{BC}] = \text{Concentration of black carbon (soot)}$$

$$[\text{Smoke}] = [\text{K}] - 0.6[\text{Fe}]$$

$$[\text{Seasalt}] = 2.54[\text{Na}]$$

$$[\text{Sulphate}] = 4.125[\text{S}]$$

The reconstructed mass (RCM) is based on the fact that the six composite variables or 'pseudo' sources given in equation A1.11 are generally the major contributors to fine and coarse particle mass and are based on geochemical principles and constraints. The [Soil] factor contains elements predominantly found in crustal matter (Al, Si, Ca, Fe, Ti) and includes a multiplier to correct for oxygen content and an additional multiplier of 1.16 to correct for the fact that three major oxide contributors (MgO, K₂O, Na₂O) carbonate and bound water are excluded from the equation. Organic carbon concentrations [OC] were estimated using equation A1.12, where PESA was used to determine the hydrogen concentration on filters. In this case, total hydrogen on the filter was assumed to be comprised mainly of H from organic material and ammonium sulphate (assuming sulphate is in fully neutralised form) and therefore organic content (designated [OMH]) was calculated from total H by the following equation (Cohen, 1999; Malm et al., 1994):

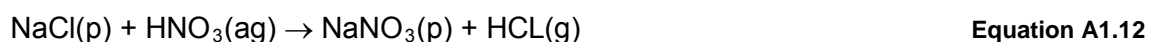
$$[\text{OMH}] = 11([\text{H}] - 0.25[\text{S}])$$

Equation A1.11

Equation A1.12 assumes that average particulate organic matter is composed of 11% H, 71% C, and 20% O by weight. Where a measure of [OC] was not available, it was assumed that it composed part of the 'remaining mass' (the difference between RCM and gravimetric mass) that includes water and nitrates as major components (Cahill et al., 1989).

[BC] is the concentration of black carbon, measured in this case by light reflectance/absorbance. [Smoke] represents K not included as part of crustal matter and tends to be an indicator of biomass burning.

[Seasalt] represents the marine aerosol contribution and assumes that the NaCl weight is 2.54 times the Na concentration. Na is used as it is well known that Cl can be volatilised from aerosol or from filters in the presence of acidic aerosol, particularly in the fine fraction via the following reactions (Lee et al., 1999):



Alternatively, where Cl loss is likely to be minimal, such as in the coarse fraction or for both size fractions near coastal locations and relatively clean air in the absence of acid aerosol, then the reciprocal calculation of [Seasalt] = 1.65[Cl] can be substituted, particularly where Na concentrations are uncertain.

Most fine sulphate particles are the result of oxidation of SO₂ gas to sulphate particles in the atmosphere (Malm et al., 1994). It is assumed that sulphate is present in fully neutralised form as ammonium sulphate. [Sulphate] therefore represents the ammonium sulphate contribution to aerosol mass with the multiplicative factor of 4.125[S] to account for ammonium ion and oxygen mass (i.e., (NH₄)₂SO₄ = ((14 + 4)2 + 32 + (16x4)/32)).

Additionally, the sulphate component not associated with seasalt can be calculated from equation A1.15 (Cohen 1999):

$$\text{Non-seasalt sulphate (NSS-Sulphate)} = 4.125 ([S_{\text{tot}}] - 0.0543[\text{Cl}]) \quad \text{Equation A1.14}$$

Where the sulphur concentrations contributed by seasalt are inferred from the chlorine concentrations, i.e., [S/Cl]seasalt = 0.0543 and the factor of 4.125 assumes that the sulphate has been fully neutralised and is generally present as (NH₄)₂SO₄ (Cahill, Eldred *et al.* 1990; Malm, Sisler *et al.* 1994; Cohen 1999).

The RCM and mass closure calculations using the pseudo-source and pseudo-element approach are a useful way to examine initial relationships in the data and how the measured mass of species in samples compares to gravimetric mass. Note that some scatter is possible because not all aerosols are necessarily measured and accounted for, such as all OC, ammonium species, nitrates and unbound water.

As a quality assurance mechanism, those samples for which RCM exceeded gravimetric mass or where gravimetric mass was significantly higher than RCM were examined closely to assess gravimetric mass and IBA data. Where there was significant doubt either way, those samples were excluded from the receptor modeling analysis. The reconstructed mass calculations and pseudo source estimations are presented in the appendices at the end of this report.

A1.4.2 Dataset preparation

Careful preparation of a dataset is required because serious errors in data analysis and receptor modeling results can be caused by erroneous individual data values. The general methodology followed for dataset preparation was as recommended by (Brown and Hafner, 2005). For this study, all data were checked for consistency with the following parameters:

1. Individual sample collection validation;
2. Gravimetric mass validation;
3. Analysis of RCM versus gravimetric mass to ensure RCM < gravimetric;
4. Identification of unusual values including noticeably extreme values and values that normally track with other species (e.g., Al and Si) but deviate in one or two samples. Scatter plots and time series plots were used to identify unusual values. One-off events such as fireworks displays, forest fires or vegetative burn-offs may affect a receptor model as it is forced to find a profile that matches only that day;
5. Species were included in a dataset if at least 70% of data was above the LOD and signal-to-noise ratios were checked to ensure data had sufficient variability. Important tracers of a source where less than 70% of data was above the LOD were included but model runs with and without the data were used to assess the effect;
6. For PCA, % errors and signal-to-noise ratios were used as a guide as to whether a species was too 'noisy' to include in an analysis.

In practice during data analyses, the above steps were a reiterative process of cross checking as issues were identified and corrected for, or certain data excluded and the effects of this were then studied.

A1.4.2.1 PMF data matrix population

The following steps were followed to produce a final dataset for use in the PMF receptor model (Brown and Hafner, 2005).

Below detection limit data: For given values, the reported concentration used and the corresponding uncertainty checked to ensure it had a high value.

Missing data: Substituted with the dataset median value for that species.

A1.4.2.2 PMF uncertainty matrix population

Uncertainties can have a large effect on model results so that they must be carefully compiled. The effect of underestimating uncertainties can be severe, while overestimating uncertainties does not do too much harm (Paatero and Hopke, 2003).

Uncertainties for data: Data was multiplied by % fit error provided by IBA analysis to produce an uncertainty in ng m^{-3} .

Below detection limit data: Below detection limit data was generally provided with a high % fit error and this was used to produce an uncertainty in ng m^{-3} . Zero data was given a corresponding uncertainty value of $4 \times \text{LOD}$.

Missing data: Uncertainty was calculated as $4 \times$ median value over the entire species dataset.

BC: Because of high mass values for BC, the uncertainties were generated by multiplying mass values by a factor of four to down-weight the variable.

PM gravimetric mass: Uncertainty given as $4 \times$ mass value to down-weight the variable.

Reiterative model runs were used to examine the effect of including species with high uncertainties or low concentrations. In general it was found that the initial uncertainty estimations were sufficient and that adjusting the 'additional modelling uncertainty' function accommodated any issues with modelled variables such as those with residuals outside ± 3 standard deviations.

A2.0 APPENDIX 2: CORRELATION PLOTS

Figure A2.1 presents an elemental correlation plot.

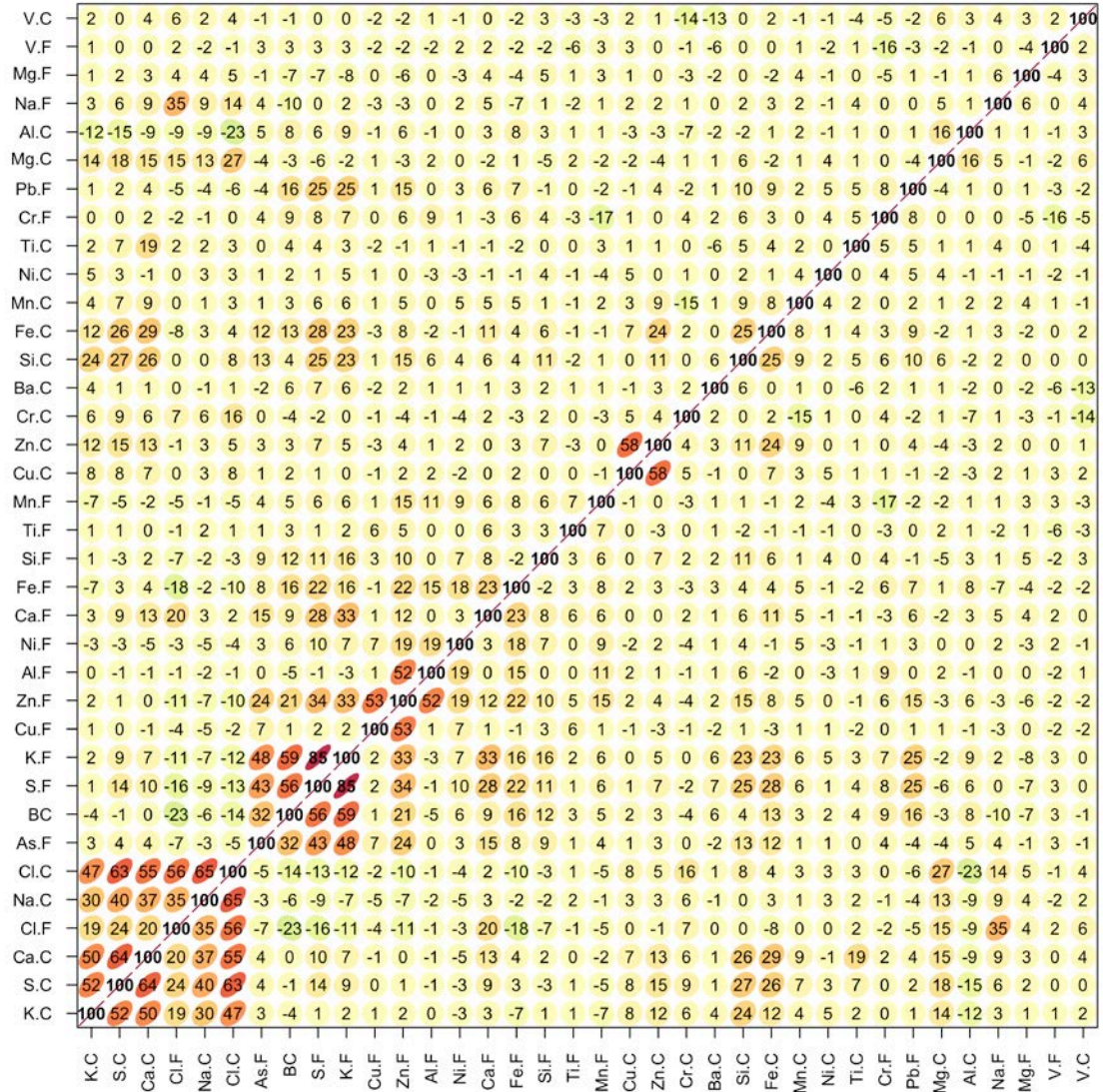


Figure A2.1 Elemental correlation plot.



www.gns.cri.nz

Principal Location

1 Fairway Drive
Avalon
PO Box 30368
Lower Hutt
New Zealand
T +64-4-570 1444
F +64-4-570 4600

Other Locations

Dunedin Research Centre
764 Cumberland Street
Private Bag 1930
Dunedin
New Zealand
T +64-3-477 4050
F +64-3-477 5232

Wairakei Research Centre
114 Karetoto Road
Wairakei
Private Bag 2000, Taupo
New Zealand
T +64-7-374 8211
F +64-7-374 8199

National Isotope Centre
30 Gracefield Road
PO Box 31312
Lower Hutt
New Zealand
T +64-4-570 1444
F +64-4-570 4657